

THE EFFECTS OF GOLD MINING ON MICROBIOME COMPOSITION IN A
FRESHWATER ECOSYSTEM

A Thesis

Presented to

The Faculty of the Department of Biological Sciences

Sam Houston State University

In Partial Fulfillment

of the Requirements for the Degree of

Master of Science

by

Caroline Elise Obkirchner

May, 2019

THE EFFECTS OF GOLD MINING ON MICROBIOME COMPOSITION IN A
FRESHWATER ECOSYSTEM

by

Caroline Elise Obkirchner

APPROVED:

Madhusudan Choudhary, PhD
Thesis Co-Director

Carmen G. Montaña-Schalk, PhD
Thesis Co-Director

Anne R. Gaillard, PhD
Committee Member

Diane L. H. Neudorf, PhD
Committee Member

John Pascarella, PhD
Dean, College of Science and Engineering
Technology

ABSTRACT

Obkirchner, Caroline Elise, *The effects of gold mining on microbiome composition in a freshwater ecosystem*. Master of Science (Biology), May, 2019, Sam Houston State University, Huntsville, Texas.

Mercury (Hg) contamination of freshwater ecosystems due to gold mining activities is a source of human health, environmental, and food security problems around the world. In Guyana, South America, it is estimated that 80 tons of mercury is expelled into the environment due to gold mining processes each year. Once in the aquatic environment, mercury undergoes methylation by microorganisms including sulfate reducing bacteria (SRB) iron reducing bacteria (IRB), firmicutes, and methanogens that have capabilities for mercury methylation. Methyl mercury (MeHg) is a neurotoxin, and it bioaccumulates and biomagnifies through the food chain leading to high MeHg concentrations in the tissues of fish ordinarily consumed by people. This places them at risk of MeHg poisoning and health related problems including ataxia, organ damage and birth defects. Although the effects of biomagnification and bioaccumulation are previously documented, further characterization of the microbiome existing in these aquatic systems is necessary to fully comprehend the nature of microbial mercury methylation. This study tested the following hypotheses. Hypothesis 1: Certain physiochemical and habitat characteristics will be significantly different between gold mined and non-mined sites. Hypothesis 2: The concentrations of gold (Au), arsenic (As), and sulfur (S) in sediments will be significantly different between gold mined and non-mined sites. Hypothesis 3: The concentration of Hg and MeHg in sediments at gold-mined sites will be higher than at non-mined sites. Hypothesis 4: The composition of the microbiome structure will be significantly different between gold mined and non-mined

sites. Results indicate that certain physical (e.g., temperature, total dissolved solids (TDS), and turbidity), chemical (pH and electrical conductivity) and habitat (% macrophytes) were significantly different between gold mined and non-mined sites (Mann-Whitney U test, p -value <0.05); however, because of the complex nature of neotropical rivers, the significant difference in specific parameters cannot be explained simply due to presence of mining activity. Elemental analysis revealed that there is a higher concentration of Au, As, Hg and MeHg in soil sediments collected from gold-mined sites than found at non-mined sites (Mann-Whitney U test, p -value <0.05). Results also revealed significant differences in microbial community structure between mined and non-mined sites on various taxonomic levels. *Proteobacteria* were present in greater percent relative abundance (Kruskal Wallis test, $p < 0.01$) at mined sites (46.23%) than the non-mined sites (34.23%), while *Actinobacteria* were found significantly in greater abundance (Kruskal Wallis test, $p < 0.01$) at non-mined sites (34.39%) than the mined sites (25.78%). Additionally, known bacteria, including *Geobacter* and *Desulfosporosinus* with mercury methylation capability were found in higher abundance at mined sites (Kruskal Wallis test, $p<0.05$). In conclusion, the composition of microbiome was significantly different between mined and non-mined sites, and mined sites had higher abundance of confirmed mercury methylators, which are likely to be contributing to the production of MeHg at three gold-mined sites.

KEY WORDS: Gold mining, Microbiome, Mercury, Methylmercury, Hg, MeHg, neotropical river, sediment microbiome.

DEDICATION

I would like to dedicate this thesis to my family, especially to my father, Stuart mother Kelly, sisters Gabby, Kelly, and Maura, and brother Kenneth. I would particularly like to thank my mentor Dr. Madhusudan Choudhary. I would also like to thank my partner Aris Manos. They all have helped me through this process in their own, unique and necessary way and have provided me with enduring love and support.

ACKNOWLEDGEMENTS

I would like to thank my thesis advisors Dr. Madhusudan Choudhary and Dr. Carmen Montaña-Schalk for their support and patience and for helping me grow as a scientist.

I would like to thank Mr. Elford Liverpool and his undergraduates at the University of Guyana for performing the sample collection that made this research possible.

I would also like to thank my committee members, Dr. Anne Gaillard and Dr. Diane Neudorf for their time and insights throughout this project.

Finally, I would finally like to thank Santos Gonzalez and Ibeth Caceres for their help in data collection and analysis.

TABLE OF CONTENTS

	Page
ABSTRACT.....	iii
DEDICATION.....	v
ACKNOWLEDGEMENTS.....	vi
TABLE OF CONTENTS.....	vii
LIST OF FIGURES	ix
CHAPTER	
I INTRODUCTION	1
II METHODS	16
Study site and sample collection.....	16
Elemental analysis	19
Microbiome analysis.....	22
III RESULTS AND DISCUSSION.....	29
Differences in physical, chemical, and habitat characteristics	29
Elemental analysis	36
Microbiome analysis.....	44
Future work.....	58
REFERENCES	60
APPENDIX A.....	82
APPENDIX B.....	83
APPENDIX C	84
APPENDIX D.....	85

APPENDIX E	86
APPENDIX F.....	87
APPENDIX G.....	88
APPENDIX H.....	89
APPENDIX I	90
APPENDIX J	91
VITA.....	92

LIST OF FIGURES

Figure	Page
1 Annual global total Hg distribution and deposition in 2013.....	4
2 Map depicting areas across the Guiana Shield that are impacted by gold mining (in red) and greenstone areas (in green).	6
3 Map showing the locations of 27 sample collection sites along the tributaries and main channel of the Mazaruni River in Guyana, South America.	17
4 Map showing locations of five selected sites along the tributaries and main channel of the Mazaruni River in Guyana, South America.	18
5 A schematic diagram of the 16S rRNA gene.....	22
6 Workflow diagram depicting the steps for metagenomic sequencing.	22
7 Workflow diagram depicting the steps used with QIIME2 to analyze the 16S sequencing data.	26
8 Physical parameters that were significant at sampling sites (red= mined sites, green = non-mined sites).....	30
9 Chemical parameters that were significant at sampling sites (red = mined sites, green = non-mined sites).	33
10 Habitat parameter that was significant at sampling sites (red=mined sites, green=non-mined sites).....	36
11 Concentrations of elemental analysis performed in fluvial sediments (red=mined sites, green=non-mined sites).....	37
12 Total mercury concentrations in the study sites (red = mined sites, green = non-mined sites).....	41

13 Comparison of average mercury (red) and methyl mercury (blue) concentrations.	43
14 Length distribution of 16S rDNA sequences.	44
15 Rarefaction curve of alpha diversity in fluvial sediment samples collected in triplicates from three mined and two non-mined sites (n=15).	45
16 Box plots of observed OTUs for three mined and two non-mined sites.	46
17 Principal coordinate analysis (PCoA) plot of the weighted UniFrac distances at three mined (red) and two non-mined (green) sites.	47
18 Venn diagram of unique and shared OTUs found at mined and non-mined sites.	48
19 Taxonomic distribution of top 20 most abundant phyla at mined and non-mined sites.	50
20 Scatterplot relating mercury (Hg) concentration and percent abundance of γ -proteobacteria.	52
21 Taxonomic distribution of top 20 most abundant family groups at mined and non-mined sites.	53
22 Taxonomic distribution of top 20 most abundant genera at mined and non-mined sites.	56
23 Estimated average (\pm SD) abundance of genera that contain the <i>hgcAB</i> gene cluster.	59

CHAPTER I

Introduction

Heavy metal contamination is a threat to both human and environmental health. The general collective term “heavy metal” may refer to the metals and metalloids that have an atomic density greater than 4 g/cm^3 , or the metal or metalloids with densities at least 5 times greater than water (Hutton and Symon, 1986; Battarbee et al., 1990). Additionally, heavy metals are defined as elements that have an atomic weight between 63.546 and 200.590 (Kennish, 1991). A heavy metal is also defined as any metallic element that has a relatively high density and is toxic at low concentrations (Lenntech, 2004). A few heavy metals that meet the above criteria include mercury (Hg), arsenic (As), cadmium (Cd), lead (Pb), copper (Cu), and chromium (Cr) (Järup, 2003; Nagajyoti et al., 2010; Barakat, 2011). The heavy metals that occur naturally in the earth’s crust vary in concentration and combination across geographic regions and undergo geochemical cycling, and thus, are never created nor destroyed. In the crust, these heavy metals exist as their ores in various chemical forms, and they are recovered by mineral processing operations (Peplow, 1999). Additionally, some heavy metals, such as cobalt (Co), copper (Cu), zinc (Zn) and manganese (Mn) are trace elements because they benefit the growth and development of living organisms at low concentrations. Some of these trace elements like zinc (Zn) and copper (Cu) are cofactors and activators of specific enzymatic reactions (Mildvan, 1970) and are involved in processes like redox reactions, electron transfer and nucleic acid metabolism (Sharma & Agrawal, 2005). Even though certain heavy metals can have biologically beneficial properties to the organism, if not

maintained within limited concentrations, they can result in toxicity (Fosmire, 1990; Nolan, 2003).

Heavy metals such as Hg, Cd, As, and Pb, have no such biologically beneficial properties for humans, and intake of any of these even at low concentrations is highly detrimental and potentially fatal (Holum, 1983; Fosmire, 1990). Still, these heavy metals, among others, are introduced into the environment through anthropogenic sources such as mining and smelting operations, agricultural use of metals and metal containing compounds, and coal burning in power plants (Nriagu 1989; Fergusson, 1990; He 2005). In addition, other sources of human exposure to heavy metals are due to their increased use in pharmaceutical applications (Bradl, 2002).

Hg contamination poses serious health threats due to environmental or occupational exposure and is ranked the third most toxic element to human health by the United States Government Agency for Toxic Substances and Disease Registry (ATSDR) (Budnik & Casteleyn, 2018). Mercury is found naturally in trace amounts in igneous rocks and can exist in numerous forms including elemental mercury (Hg^0), inorganic mercury (Hg^{2+}), and organic compounds such as methylmercury (MeHg) and ethyl mercury. Mercury is a heavy metal that is also a dangerous neurotoxin and is commonly introduced into the environment by natural sources such as volcanic emissions (in the form of elemental mercury) (Nriagu & Becker, 2003), degassing from soils, rock weathering and emissions from the ocean (Pirrone et al., 2001), and deposits of the red mineral cinnabar (HgS) (Budnik & Casteleyn, 2018). Anthropogenic sources of mercury include power plants, smelters, incinerators, cement plants, chemical plants (Pirrone et al., 2010), coal burning plants (Pacyna et al., 2006) and gold mining activities (Lacerda,

1995; Veiga et al., 2006). Due to the complex nature of the biogeochemical Hg cycle, it is difficult to correctly determine an accurate extent of human health and environmental risks and point sources are not always identifiable nor solely responsible (Eagles-Smith et al., 2018). Regardless of the anthropogenic or natural source, once mercury is emitted into the atmosphere, it can be deposited into aqueous environments by wet and dry depositions and are re-volatilized to the atmosphere (Kim et al., 2012; Dittman et al. 2010 Demers et al. 2007, and Filippelli et al., 2012).

Although there are numerous sources of mercury contamination, the foremost source is due to artisanal and small-scale gold mining. Artisanal and small-scale gold mining produces less than 1000,000 tons of gold per year for profit and does not follow conventional ecological and engineering principles of mining and instead uses rudimentary techniques for mineral extraction (Seccatore et al., 2014). This form of mining is responsible for 17% - 20% of official gold production in the world and around 380-450 tons of gold are produces annually using this method by around 16 million artisanal miners worldwide (U.S Geological Survey 2013, Seccatore et al., 2014). Artisanal and small-scale gold mining is practiced worldwide and is estimated to contribute 1608 tons of Hg to the environment yearly, and thus affects countries across the spatial and socio-economic spectrum (Veiga et al., 2014). The distribution and concentration of mercury pollution across the world is visualized in Figure 1.

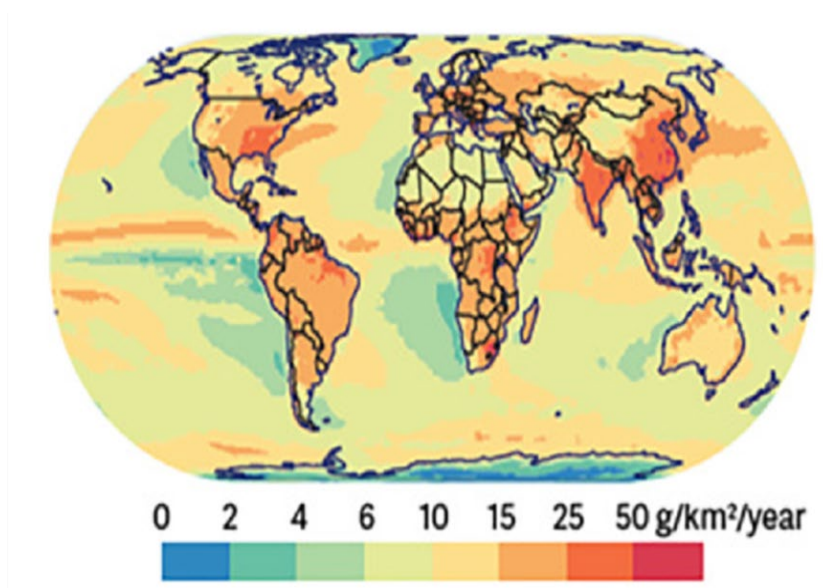


Figure 1. Annual global total Hg distribution and deposition in 2013. The different colors represent their corresponding concentrations of Hg (Source: UNEP, 2013).

Artisanal and small-scale gold miners use mercury to extract gold from gold bearing ore via amalgamation. Although this process regularly exposes both the miner and the environment to mercury, the process is still immensely popular and widely used because mercury is relatively inexpensive and readily accessible through both legal and illegal channels (Spiegel et al., 2006). The popularity of mining with mercury is problematic because, while the mining operation may only last 15 years, studies indicate metal contamination can persist in the mining area and surrounding environment for hundreds of years (Duruibe et al., 2007). However, mercury use in gold mining is by far not a novel practice. In fact, mercury use in mining has been employed since 2700 B.C.E by the Phoenicians and Carthaginians in Spain. There, the practice became well known due to the Romans in 50 C.E, although the use of mercury was eventually banned by the Romans, likely due to a health crisis caused by the use mercury (Lacerda 1997; Salomons, 1998, Rojas et al. 2001). The use of mercury in gold mining is so ubiquitous it

has been speculated that without mercury, it is likely there would not have been any gold rushes at all (Nriagu & Wong, 1997).

Mercury contamination due to mining activities is globally pervasive and occurs in many countries. For example, certain villages in China known to be historical mining sites exhibit high Hg concentrations in their soils and vegetables that surpass tolerance limits and thus places the local population at increased risk of mercury poisoning (Qui, et al., 2008). Also, in North America, more specifically California, mercury has been used extensively in the extraction of gold from alluvial deposits as late as the 1960s, and fish from the Bear-Yuba watershed for example, display high levels of Hg (Church et al., 2005). A large amount (~260, 000 tons) of mercury was released into the biosphere due to mining activities across the world. Current increases in the price of gold as well as worsening socioeconomic conditions in many developing countries, including South America, have resulted in the growth artisanal and small-scale mining, which involves more 10-19 million people of which 4-5 million are women and children (Eisler, 2004; Esdaile & Chalker, 2018). Impacts from placer gold mining operations in rivers of the Amazon and Suriname have resulted in habitat transformation, consequently shifting fish diversity and community composition (Miller et al. 2003; Mol & Ouboter 2004; Barbieri & Gardon 2009; Brosse et al. 2011). Miners expel and estimated 80 tons of mercury across the Guianas each year (Legg et al., 2015) in the northeast region of South America known as the Guiana Shield. The Guiana Shield has a surface area of nearly 900,000 Km² and most was formed during prolonged periods of powerful magmatism and metamorphism, and is considered Precambrian terrane (Voicu et al., 2001). The Guiana Shield spans across multiple countries including Guyana, Suriname, and French Guiana

and contains vast deposits of gold which are currently and have historically been mined by artisanal and small-scale gold miners as seen in Figure 2. In the underpopulated areas of the Guianas, artisanal and small-scale mining is the most available form of employment and has been for more than 30 years (Smith et al., 2017).

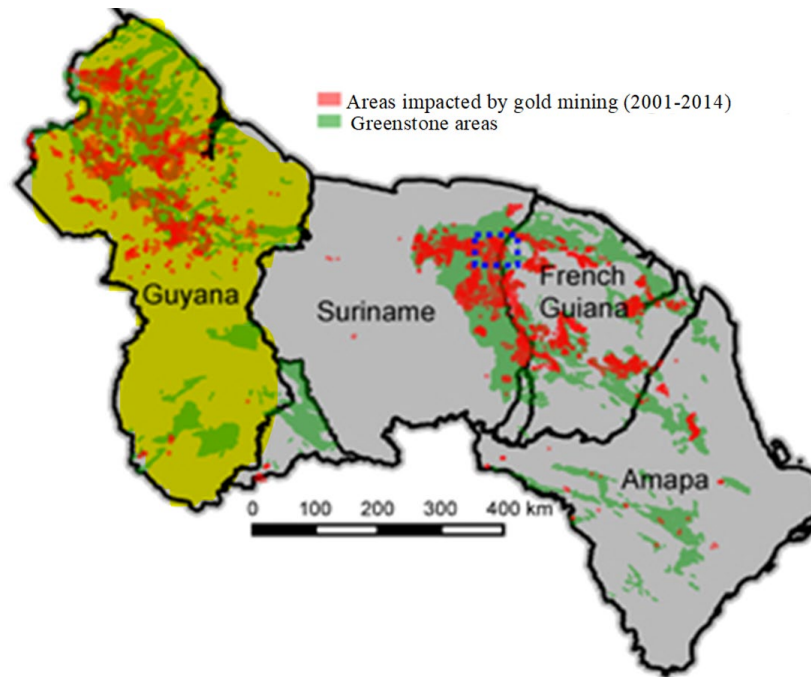


Figure 2. Map depicting areas across the Guiana Shield that are impacted by gold mining (in red) and greenstone areas (in green). Guyana is emphasized in yellow (Adapted from Dezécache et al., 2017).

The rivers within the Guiana Shield are highly diverse, containing the highest concentration of freshwater biodiversity in the world (Reis & Albert. 2011). The mercury emission from mining not only puts the vast biodiversity and high species endemism of the area at risk for mercury toxicity, but also the local human populations. Guyana, a small English country located on the Northeastern shoulder of South America, has a long history of gold mining, and recent escalation in gold extraction has led to a trend of increased deforestation and increased pollution of freshwater ecosystems (Miller et al., 2003). This small country has an area around 83,000 square miles, a population

size estimated to be 742,000, and an economy heavily dependent on natural resource extraction (Cantebury, 2016). In fact, gold is Guyana's biggest export, accounting for around 37% of exports, which is more than sugar and rice combined (Guyana Bureau of Statistics, 2010). With gold extraction being so vital to the health of the economy, it is improbable this destructive trend will cease. Due to the continuing rising price of gold, and gold mining itself being Guyana's second largest GDP component, artisanal and small-scale gold mining will continue to be a threat to human health and biodiversity unless appropriate action is taken (Rahm et al., 2015). Although Guyana's National Development Strategy (NDS) states that the country's plans for development should be guided by strict environmental considerations, the regulation of the growing gold mining industry has been lenient, and gold mining activities have caused waste pollution, river contamination through cyanide and mercury, soil erosion, deforestation, and destruction of wildlife (Roopnarine, 2002). Thus far, there are two main gold mining practices in this region, both of which are harmful: primary gold mining and alluvial gold mining. Primary gold mining involves clearing the vegetation at the site to be mined and blasting the gold bearing rock with explosives, or targeting it with high power water pumps, to create a gold containing slurry that is pumped into sluice boxes via gravel pumps (Clifford, 2001). This type of mining is also referred to as "land dredging" or "hydraulicking". Alluvial gold mining involves the use of large dredges (floating platforms) that are undertaken by individuals (miners) to dig and sift particles through sediments or sand using a sieve or the miner own hands. This form of mining was extremely popular, and its use peaked during the 1980's and 1990's, but since then has begun to decline due to widespread exhaustion of gold deposits. However, alluvial

mining is still practiced Clifford, 2011). The dredges used in alluvial mining are equipped with rotating drums and pumps that uptake the riverbed material, which consists of a sand cement mixer housing the gold containing sediments; the resulting mercury containing tailings end up returning to the river (Balzino et al., 2015). The resulting mercury-gold amalgam consists of 60% Au and 40% Hg; thus, the remaining mercury must be removed from the mercury-gold amalgam (Veiga et al., 2013). To do this, the amalgam is burned in a furnace which results in the release of dangerous mercury vapors to the atmosphere around burning sites (Balzino et al., 2015). This method is often inefficient, and the use of mercury is hazardous to the health of the miners and nearby populations of people, and results in mercury contamination of both aquatic and atmospheric environments. Dredges are very important for the expansion of small-scale mining operations in Guyana, and subsequently the number of dredges working Guyana's rivers has doubled from 2004 to 2008; and around 900 new dredges were added to the rivers at the end of 2008 (Thomas, 2009).

There are two forms of mercury that are relevant in these instances. The first form, inorganic mercury, is the result of the oxidation of elemental mercury that is used for amalgamation purposes in the mining process and subsequently released into the water bodies after amalgamation. Once in the lotic system, the inorganic mercury is then available to be methylated by microbes, and subsequently becomes methylmercury (MeHg) which is the species of mercury that is readily adsorbed by plants, microorganisms, soil microorganisms, and fauna (Garcia-Sanchez & Szakova 2016). This is important because the chemical speciation of mercury directly influences its mobility and toxicity. MeHg is the speciation of the most concern because once it enters the

aquatic ecosystems it bioaccumulates and biomagnifies through each trophic level of the aquatic food web, with higher concentrations in fishes and humans (Hall et al. 1997; Barbosa et al. 2003; Chumchal et al. 2008; Barbieri & Gardon 2009). Bioaccumulation occurs when the concentration of a substance in an organism increases over time, while biomagnification occurs when the concentration of a substance increases with each subsequent trophic level (Pouilly et al., 2013). Metal mercury, the inorganic form of mercury, is considered less toxic and does not bioaccumulate, while MeHg is of major concern because it bioaccumulates and is extremely neurotoxic. MeHg can bioaccumulate in fishes because it binds to the amino acids in fish muscle, which cannot be removed through cooking techniques, leading to subsequent bioaccumulation in the organisms consuming the contaminated fish (Morgan et al., 1997). Because of the ability of MeHg to bioaccumulate and biomagnify through aquatic food webs, populations whose main protein source is fish are at increased risk of MeHg exposure. Therefore, the predominant exposure of MeHg to humans is through the consumption of seafood. One of the reasons this route of exposure is cause for concern is because it is estimated 400 million women of reproductive age across the world depend on seafood for at least 20% of their animal protein intake, and MeHg exposure to developing fetuses can cause brain and nervous system damage (Grandjean et al., 1997; Clarkson et al., 2006). An infamous example of the extensive damage mercury contamination can cause is the health crisis that occurred in Minamata Bay, Japan, during the 1950s and 1960s. There, a chemical company named Chisso systematically released mercury effluent into the bay that was commonly used for fishing. After bioaccumulation and biomagnification, this led to severe MeHg poisoning via the consumption of contaminated seafood in the bay. It

caused the local population to develop what is now known as “Minamata disease”, a disease named after this incident and characterized by symptoms such as paresthesia, ataxia, dysarthria, and children (that were exposed in utero) born with debilitating conditions (Yorifuji et al., 2017). This has not been the last incidence of large-scale mercury contamination resulting in MeHg poisoning. In subsistence fishing populations, specifically in the Amazon, incidence of mild mental retardation has been studied and recorded as 17.4 cases per 1000 babies (Poulin & Gibb, 2008). A study assessing the Hg levels of one at-risk population, the indigenous Wayana of southeast Suriname, is an example of the negative impact of mercury contamination on human health. When Hg levels of the Wayana were measured, they were found to be significantly higher than the World Health Organization limit (0.5 mg Hg/kg), and neurotoxic effects were observed (Peplow, 2014). In Guyana, it is estimated that the environmental contamination from gold mining places 750,000 inhabitants, including 40,000 interior Amerindians, at direct risk, for many directly depend on the environment for food and living (Roopnarine, 2002). The soluble nature of MeHg is part of what makes it so dangerous to human health. Once in the organism, the MeHg is free to combine with L-type cysteine to create L-cysteine-methylmercury conjugates that can be distributed to all tissues, including the brain, because methylmercury conjugates are regarded akin to the L-type neutral amino acid, methionine (Sakamoto et al., 2018). This means MeHg could accumulate in the kidney, liver, and brain in addition to other tissues, resulting in symptoms such as ataxia, tremors, blindness, pulmonary edema, nervous system disease, kidney damage and brain damage (Tchounwou et al., 2012; Ayangbenro & Babalola, 2017). The MeHg that crossed the blood brain barrier will, after time, be metabolized to mercuric Hg which can

evoke immunological reactions, leading to further health complications (Bjorklund et al., 2017). Other health effects of MeHg exposure include cardiovascular atherosclerosis, myocardial infarction, heart rate variability and hypertension (Guallar et al., 2002; Buchanan et al., 2015). Further studies have demonstrated a correlation between MeHg exposure and increased risk of neuro developmental disorders such as ASD, ADHD, and altered language/speech skills (Landrigan et al., 2002). Globally, all diseases caused after mercury pollution are a large portion of pollution-related diseases, which cause millions of premature deaths (Steckling et al., 2017). In summary, mercury pollution due to artisanal and small-scale gold mining is extensive and has serious impacts on environmental and human health.

Therefore, it is important to study the microbial methylation of mercury because of its implications on human health. Inorganic mercury is most commonly methylated via anaerobic microbes such as sulfate reducing bacteria (SRB) and iron reducing bacteria (IRB) in soil sediments and bottom waters under anoxic environments (Gilmour et al., 1992; Kerrin et al., 2006). However, it is important to note that the ability to methylate Hg is not ubiquitous among SRB and IRB (Kerrin et al., 2006). SRB are a physiological group of bacteria that consist of around 220 genera and are distributed among diverse phylogenetic groups such as *δ-proteobacteria*, *Firmicutes*, and *Archaea* (Castro et al., 2000; Barton and Fauque, 2009). SRB are characterized as bacteria that can reduce sulfate to hydrogen sulfide (Widdel, 1988). IRB couple the oxidation of H² or organic substrates to the reduction of ferric iron (Fredrickson and Gorby, 1996). Members of SRB such as *Desulfovibrio desulphuricans* and IRB such as *Geobacter sulphurreducens* methylate inorganic mercury. Bacterial mercury methylation appears to be linked to the

Acetyl-CoA pathway (possibly by this pathway supplying the methyl group to Hg methylating enzymes (Berman et al., 1990) although it has been found that some SRB do not use the Acetyl-CoA pathway for mercury methylation (Ekstrom et al., 2003). However, the bacterial genes involved in production of MeHg have recently been identified. These genes, *hgcA* and *hgcB*, encode a corrinoid dependent protein and an associated ferredoxin protein, respectively, and have been detected in species additional to SRB and IRB, such as methanogenic, acetogenic, and cellulolytic microbes (Gilmour et al., 2013). It is suggested that *hgcA* encodes the corrinoid protein (HgcA) that donates a methyl group to Hg (II) and also has a transmembrane domain that could be involved with the uptake of Hg (II) and or the release of MeHg from the cell (Lin et al., 2014; Date et al., 2019). *hgcB* encodes the iron-sulfur cluster protein (HgcB) which is proposed to provide electrons to the cobalt ion of HgcA, which is important to maintain the cycle of methylation (Smith et al., 2015). More specifically, using density functional theory calculations with a model of HgcA has demonstrated that there is a strictly conserved cysteine (Cys) residue that coordinates to Co (III) which enables methyl radical and methyl carbanion transfers to inorganic mercury substrates (Zhou et al., 2013). More precisely, site-directed mutagenesis of *hgcA* and *hgcB* provided further evidence the amino acid residue Cys93 in HgcA is necessary for mercury methylation and is the proposed ligand to the corrinoid cobalt (Smith et al., 2015). It has been found that uptake of mercury by SRB and IRB can occur via passive or active transport processes or by a combination of both, whereas organisms with the mercury resistance (*mer*) operon that reduces inorganic mercury to elemental mercury, exports the elemental mercury by simple diffusion (Hsu-Kim et al., 2013). When one or both genes were deleted in

Desulfovibrio desulphuricans or *Geobacter sulphurreducens* PCA, it resulted in both organisms losing their mercury methylation ability (Parks et al., 2013). In a recent meta-analysis, this gene pair was used to examine the distribution and diversity of Hg methylating microbes across various environments including soils, wetlands, marine waters and soil sediments (Podar et al., 2015). The results support that the gene pair is found in almost every anaerobic environment, except gut microbiomes of invertebrates. In fact, several species found with the *hgcAB* gene pair have been found in novel environments including methanogenic habitats (rice paddies for example) the animal gut, and environments with extreme pH and salinity (Gilmour et al., 2013). In addition to the *hgcAB* gene pair being found in the class δ -Proteobacteria within the phylum proteobacteria of SRB and IRB, it was also found within the phylum *Firmicutes* (*Clostridia*), and in *Methanomicrobia* within the phylum *Euryarchaeota* (Gilmour et al., 2013; Yu et al., 2013; Bae et al., 2014; Podar et al., 2015; Christensen et al., 2016). Due to the phylogenetically uneven distribution of Hg methylators with the *hgcAB* gene pair, it is likely that horizontal gene transfers (HGT) have occurred (Ranchou-Peyruse et al., 2009; Podar et al., 2015; Date et al., 2019). Bacteria with *hgcAB* genes are not solely of interest since bacteria do not exist as solitary entities, but instead constitute a bacterial community in which members cooperate with one another to manifest specific metabolic processes. For example, studies have shown that certain soil bacteria work synergistically to degrade plant biomass (Zhou et al., 2014). It is expected that there is some synergistic component in the microbiome of rivers affected by gold mining processes to methylate mercury. This expectation is supported by a study that determined when *Desulfovibrio desulfuricans* and *Methanococcus maripaludis* were grown together on a sulfate-free

lactate medium, mercury methylation occurred; however, MeHg was absent when the bacteria were grown individually (Pak & Bartha, 1998). This suggests the presence of more than one species of bacteria may be necessary to work in conjunction with another to methylate mercury. Subsequently, it is likely that members of the highly diverse bacterial communities of mercury contaminated neotropical rivers will cooperate to methylate mercury. It is possible and hypothesized that this mercury methylation could decrease inorganic mercury exposure to microbial communities (assuming that under certain conditions MeHg is less toxic than the elemental mercury substrate) (Regnell & Watrass, 2018). Microorganisms possess the ability to demethylate as well as methylate mercury, and both oxidative and reductive demethylation pathways have been identified (Oremland et al., 1991). Because oxidative demethylation is mediated by anaerobic bacteria, it is possible that in the same anaerobic environment both methylation and demethylation of elemental mercury could be occurring (Barkay & Poulain, 2007). Past research on the sediment microbiome of heavy metal contaminated rivers has indicated that the microbiomes acquired resistance to long term heavy metal pollution, and that genes involved with heavy-metal resistance and DNA repair were present and upregulated (Cabral et al., 2016; Chen et al., 2018). It is possible that this is true of microbiomes existing in mercury contaminated alluvial sediments, but further research is needed to identify what conditions favor and disfavor the abundance of bacteria that have the *hgcAB* gene pair at heavy metal contaminated sites.

Because of the potential adverse impact on human health, it is critical that the impacts of mercury contamination of aquatic food webs be elucidated. Thus far, few studies have been conducted in neotropical regions that examine MeHg introduction to

lotic aquatic food webs via microbial activity because the complex nature of hydrological dynamics of these systems makes predicting MeHg formation and bioaccumulation challenging. However, in Guyana, due to the bioaccumulation of mercury in fish and in fish consuming locals, this type of research is particularly relevant, applicable, and necessary. The following hypotheses will be tested using data collected from the Mazaruni River, Guyana, in South America.

Hypothesis 1. Several physiochemical and habitat characteristics will be significantly different between gold mined and non-mined sites

Hypothesis 2. The concentrations of gold (Au), arsenic (As), and sulfur (S) in sediments will be significantly different between gold mined and non-mined sites.

Hypothesis 3. The concentration of mercury (Hg) and methyl mercury (MeHg) in sediments at gold mined sites will be higher than at non-mined sites.

Hypothesis 4. The composition of microbiome structure will be significantly different between gold mined and non-mined sites.

CHAPTER II

Methods

Study site and sample collection

Study site. The Mazaruni River in Guyana (South America) was chosen as the study site because previous and more current literature suggest that heavy gold mining operations have been performed there (Alofs et al., 2014). Furthermore, studies conducted by Miller et al. (2003) suggest anthropogenic sources like gold mining activities are the cause of a majority of Hg contamination found in alluvial sediment deposits within the Mazaruni River basin.

Collection of water and soil samples. A total 81 soil sediment and water samples were collected from 27 sites in December 2017, as shown in Figure 3, along the tributaries and main channel of the Mazaruni River. These 27 sites included 17 active gold mining (mined) and 10 non-mining (non-mined) sites. Geographic coordinates of the 27 sites are provided in Appendix A. Three replicates were independently collected from each site and designated as replicates, A, B, and C. Soil sediment samples were collected from the river bed by extracting the sediments approximately 10 cm deep from the surface, after which they were placed into a Ziploc bag and stored temporarily in a cooler ($\pm 10^{\circ}\text{C}$) prior to its transportation to the cold room (4°C) at the laboratory at Sam Houston State University (SHSU). The concentrations of gold, arsenic, sulfur, and mercury were determined for all 81 samples. However, due to the costs of methylmercury and microbiome analyses, 15 samples from only five sites, as shown in Figure 4, were examined for the concentration of MeHg and microbiome analysis. Geographic coordinates for the 5 selected sites are provided in Appendix B.

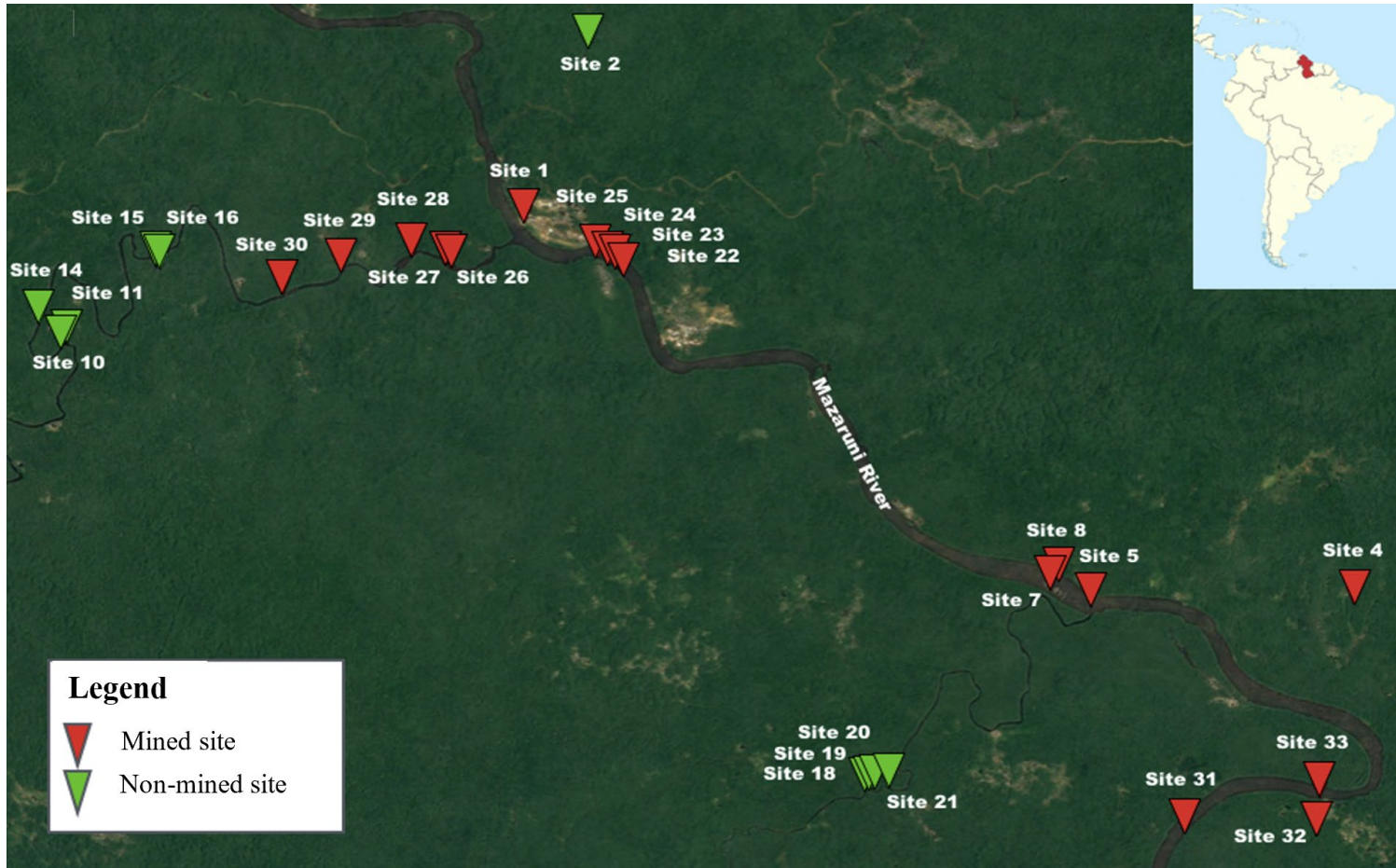


Figure 3. Map showing the locations of 27 sample collection sites along the tributaries and main channel of the Mazaruni River in Guyana, South America. Gold mined, and non-mined sites are denoted in red and green triangles, respectively.



Figure 4. Map showing locations of five selected sites along the tributaries and main channel of the Mazaruni River in Guyana, South America. Gold mined, and non-mined sites are denoted as red and green triangles, respectively. Samples from these five sites were analyzed for methylated mercury and microbiome analyses.

Physical (depth, water temperature, turbidity, total dissolved solids, silt, sand, pebbles, gravel, cobbles, rocks, and riptides), chemical (pH, electric conductivity, dissolved oxygen), and biotic/habitat (percentage distribution of trees, shrubs, grass, macrophytes, leaf litter, woody debris) parameters were recorded at each site.

Elemental analysis

Inductively coupled plasma optical emission spectroscopy (ICP-OES).

Elemental analysis of the soil samples was conducted at the Texas Research Institute for Environmental Studies (TRIES) at SHSU. The concentration of Arsenic (As), Iron (Fe) and Gold (Au) was determined by using Inductively Coupled Plasma Optical Emission Spectroscopy (ICP-OES). First, 20 g of each sample was dried at 65°C for three days. Each 0.5 g dried sample was loaded into a 50 mL digtube containing 2.5 mL of HNO₃ and 2.5 ml of H₂O. The tube was then heated at 95°C for 10 minutes. Next, 2.5 mL of more HNO₃ was added to each tube, and then these tubes were heated for two hours at 95°C. Samples were then kept at room temperature to cool, and 50 mL of deionized water was further added to these tubes. The tubes were then capped and inverted to mix for the digestion. Samples were loaded into the sampling rack of the machine for analysis. Standards for each of these elements were also prepared with the following concentration range 0.0, 1, 10, 100, 1000 µg/mL.

Multiple isotope ratio analysis using dynamic flash combustion. The FLASH EA 2000 Organic Elemental Analyzer was used to determine the concentration of Sulfur (S). Fifteen mg of each dried soil sample was placed into a tin capsule. Sulfur is usually present in soils as sulfate ions; for this reason, 5 mg of vanadium pentoxide (V₂O₅) was added to each capsule to completely convert inorganic sulfur to sulfur dioxide. These

capsules were then loaded into the FLASH EA 2000 Organic Elemental Analyzer. This system individually drops capsules into a superheated reactor where flash combustion causes a conversion of the sample into elemental gases, which was then registered by a thermal conductivity detector.

Mercury analysis using cold vapor atomic absorption spectroscopy

(CVAAS). To determine the concentration of total mercury in the soil samples, cold vapor atomic absorption spectroscopy was performed using the Millennium Merlin Mercury Analyzer. Samples were prepared using 1g of each dried sample in a 50 mL digtube. Next, 16 mL of aqua regia (3:1 ratio of HCl and HNO₃) was added to each tube and refluxed for 10 minutes at 95°C. After allowing the samples to cool, the samples were filtered. The filtrate was transferred to falcon tubes where it was then diluted to 25 mL using water. After dilution, 3 mL of KBrO₃/KBr and 2.5 mL of HCl were added to each tube, and the samples were allowed to digest for 15 minutes. After digestion, 100 µL of ClH₄NO (Hydroxylamine hydrochloride) was added, and the tubes were capped and inverted to mix a few times. Afterwards, the samples were loaded into the Merlin Mercury Analyzer. The Merlin Analyzer determines the concentration of total mercury of the sample by pumping or injecting the sample and 2% stannous chloride (SnCl₂) into a gas liquid separator. There, argon gas is added to the released mercury vapor. The mercury vapor is then carried by the argon gas to an atomic absorption optical cell where the mercury absorbs light at 253.7 nm in logarithmic proportion to the concentration of mercury in the sample (EPA, 1994). From this, the detector measures the total mercury concentration of each sample.

Methyl mercury analysis using gas chromatography cold vapor atomic fluorescence spectroscopy (GC-CVAFS). Extracted sediment samples were analyzed for methyl mercury using GC-CVAFS at Brooks Applied Labs in Seattle, Washington. Samples were extracted using methods as previously described (Bloom et al., 1997). First, 2.5 g of each sediment sample was placed into individual centrifuge tubes, and then potassium bromide (KBr), copper sulfate (CuSO_4), and methylene chloride (CH_2Cl_2) were added sequentially. KBr and CuSO_4 are used to free the organic mercury species from inorganic complexes in the sediment samples. The mixtures were kept at room temperature for an hour for the reaction to occur. Then, the centrifuge tubes were shaken using a lab shaker for an hour to completely extract any MeHg present. Afterwards the samples were centrifuged at 3000 rpm for 20 minutes to break any emulsion that could have formed. Two mL of the CH_2Cl_2 from each centrifuge tube was pipetted into its corresponding Teflon back-extraction vial which contained 10 mL of water. These vials were kept in a heating block until all CH_2Cl_2 evaporated and the MeHg back-extracted into the reagent water. The extract from each sample was then buffered to pH 4.9 and ethylated by adding sodium tetraethyl borate ($\text{C}_8\text{H}_{20}\text{BNa}$); then, deionized water was added. The vials were capped and briefly shaken. Next, the extract was purged with nitrogen gas for 20 minutes and the ethylated Hg species were collected using a sample trap containing carbotrap. The ethylated Hg species were desorbed thermally from the sample traps and separated using a gas chromatographic (GC) column, and then reduced using a pyrolytic column. The prepared samples were then loaded into the Brooks Rand Model III cold vapor atomic fluorescence spectrophotometer to determine the MeHg concentration.

Microbiome analysis

Microbiome analysis consisted of five steps; microbial genomic DNA extraction and purification, PCR amplification of 16S V3 & V4 regions (Figure 5), product purification, library preparation, and sequencing using Illumina MiSeq (Figure 6). The metagenomic sequencing was performed at LC Sciences, Houston, TX.

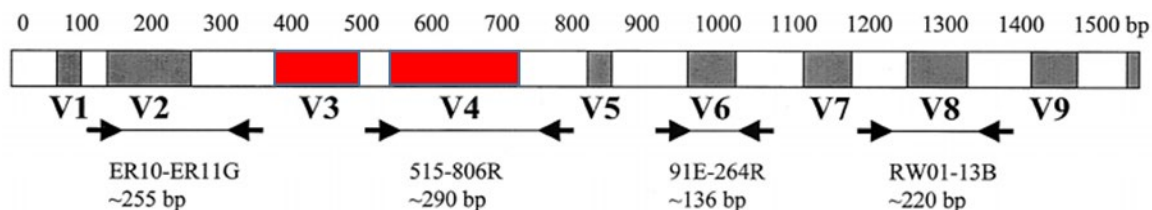


Figure 5. A schematic diagram of the 16S rRNA gene. The hypervariable regions 3 (V3) and 4 (V4) are highlighted (in red). These regions were amplified, and subsequently sequenced.

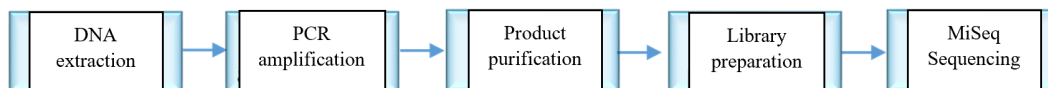


Figure 6. Workflow diagram depicting the steps for metagenomic sequencing.

DNA extraction. Microbial DNA extraction was performed using the Norgen Biotek Soil DNA Isolation Plus kit #64000. First, 250 mg of each sediment sample was added to Bead Tubes and 750 μ L of Lysis Buffer G was added. The tubes were then vortexed briefly to mix. Next, 200 μ L of Lysis Additive A was added to the tubes, and they were briefly vortexed to mix. The tubes were centrifuged for 1 minute at 14,000 RPM to pellet the protein and soil particles. The clean supernatant was transferred to a DNase-free microcentrifuge tube. Then, 100 μ L of Binding Buffer was added to the tubes, the tubes were inverted a few times, and then tubes were kept on ice for 5 minutes. The samples were then spun at 14,000 RPM for two minutes to pellet any remaining

protein and soil particles. Next, 700 μL of supernatant was transferred into a DNase-free microcentrifuge tube where 50 μL of OSR (Organic Substance Removal) solution was added to mix with the supernatant. The samples were then incubated on ice for 5 minutes, and then the lysate was spun for 2 minutes at 14,000 RPM. Then, 700 μL of cleaned supernatant was transferred to a DNase-free microcentrifuge tube, where 400 μL of Lysis Buffer QP and 550 μL of 96-100% ethanol was sequentially added. The samples were then vortexed briefly. The lysate was gently mixed with Lysis Buffer QP using a pipette, and then 600 μL of the mixed lysate was applied to the spin column and was placed in an empty centrifuge tube. The tubes along with the spin columns were centrifuged at 10,000 rpm for 30 seconds. The spin column was disassembled to discard the flow through and was then reassembled with the new collection tube. The process beginning with the addition and mixing of Lysis Buffer QP was then repeated with the remaining lysate. In order to wash the column, 500 μL of Binding Buffer B was added to the column and then centrifuged for 1 minute at 10,000 rpm. Care was taken to inspect the column for any remaining solution; if there was, the tube was spun for an additional minute. The flow through was discarded, 500 μL of Wash Solution A was added to the spin column, and the tube was then spun again for 1 minute at 10,000 rpm. The flow through was discarded and the process of additional washing with Wash Solution A was repeated. Then, the columns were spun for 2 additional minutes at 14,000 rpm to dry the resin. The collection tube was discarded, and the column was placed into a 1.7 Elution tube where 100 μL of Elution Buffer B was added to the column. The column was placed in a new centrifuge tube and incubated for 1 minute at room temperature. The tubes were then spun in a centrifuge for 1 minute at 10,000 rpm. The purified genomic DNA was stored at 2 $^{\circ}\text{C}$.

PCR amplification. The two following primers, 338F (ACTCCTACGGGAGGCAGCAG) and 806R (GGACTACHVGGGTWTCTAAT), were used to amplify the V3 and V4 regions of the 16S rDNA regions. The expected size of the amplicons was approximately 469 bp in length with some variability among differing species. PCR tubes contained 12.5 μ L Pusion Hot start flex 2x Master Mix, 2.5 μ L Forward Primer, 2.5 μ L Reverse primer, 50 ng template DNA, and 25 μ L of deionized water. Polymerase chain reaction was performed with an initial denaturing step at 98°C for 30 sec, and then for 35 cycles of amplification, each cycle consisted of denaturing at 98°C for 10 sec, annealing at 54°C for 30 sec, and extension for 72°C for 45 sec. After the first round of PCR, sequencing adapters and barcodes were added to the reaction tube for further amplification. After 35 cycles, the final extension step was at 72°C for 10 minutes. The reaction tubes were kept at 4°C for storage.

PCR Product purification. Once PCR was completed, the amplified products were confirmed using a 2% agarose gel electrophoresis. The target fragments were recovered using the AxyPrep PCR Cleanup Kit, targeting fragment sizes from 200-450 bases. To do this, 18 μ L of AxyPrep Mag PCR clean-up per 10 μ L of PCR product was used for binding DNA to Magnetic beads. The beads were then washed twice with 70% ethanol to remove salt and other contaminants. The purified PCR products were eluted from the Magnetic beads to a new tube. The PCR products were then further purified using the Quant-iT PicoGreen dsDNA Assay Kit. The newly created libraries were quantified using a Promega QuantiFluor fluorescence quantification system. To do this, first a blank was prepared by adding 200 μ L of QuantiFluor dsDNA Dye solution to an empty 0.5 mL PCR tube and the standard was prepared by adding 2 μ L of DNA standard

(100 ng/ μ L) to 200 μ L of QuantiFlour dsDNA Dye solution to empty 0.5 mL PCR tube that was then vortexed well. The samples were prepared by adding 1-20 μ L of sample to 200 μ L of QuantiFlour dsDNA Dye solution. All tubes were incubated at room temperature for 5 minutes, protected from light, then loaded into the Quantus Fluorometer. The concentration of DNA per sample was then determined. Concentrations above 2 nM were considered qualified and selected for further library preparation.

MiSeq sequencing. The qualified libraries were prepared for cluster generation and sequencing by pooling the libraries. Fully prepared libraries were then loaded into the MiSeq flow cell where clusters would be generated via isothermal cluster generation and sequencing would be performed by the pair-end synthesis method.

Sequence analysis. All raw sequences were analyzed and processed using QIIME2 2018.11 software. QIIME (Quantitative Insights into Microbial Ecology) is a software that conducts microbial community analysis. The following workflow was followed as shown in Figure 7. First, the raw sequence FASTA data was imported to QIIME2. Then the multiplexed data was demultiplexed using the q2-cutadapt plugin. In the demultiplexing process, the unique barcode sequences added during the second round of amplification are used to identify which sequences hailed from which sample. After this process, two files are generated for each site, one for the forward and one for the reverse read. The q2-cutadapt plugin was also used to remove the adapter and barcode sequences. After trimming, the plugin FLASH (Fast Length Adjustment of Short Reads) was used to merge the paired end reads into one continuous sequence tag. The sequences were then inspected for length distribution and Phred quality score. The q2-quality-filter

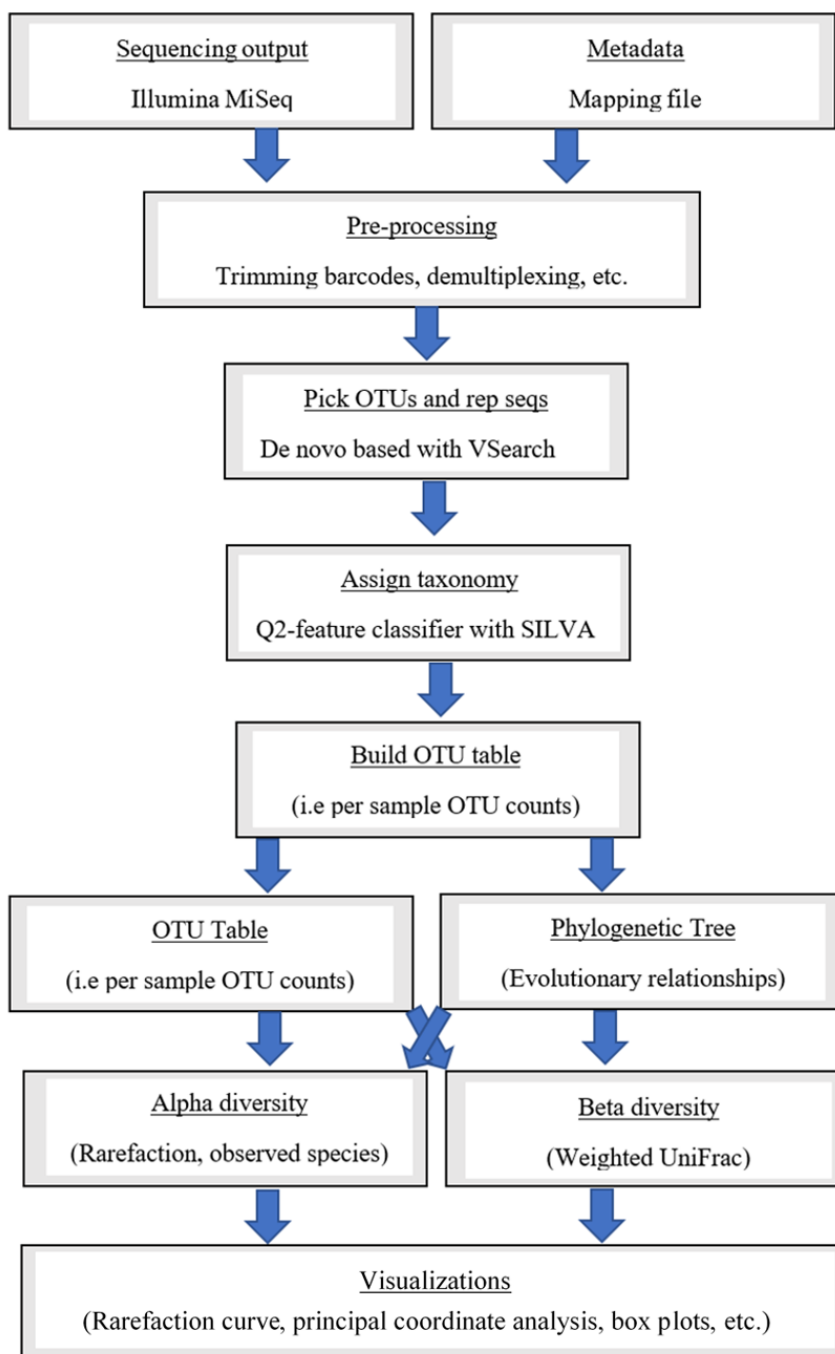


Figure 7. Workflow diagram depicting the steps used with QIIME2 to analyze the 16S sequencing data.

plugin was used to remove low quality and ambiguous reads. Chimeric sequences were removed using the q2 Vsearch plugin. Once the sequences were demultiplexed, denoised, and quality-filtered, OTU (operational taxonomic unit) clustering was performed using

the q2-Vsearch plugin, which employs a heuristic centroid-based algorithm to cluster the sequences. The sequence similarity threshold was assigned as 0.97 with the identity (id). This groups the sequences into OTUs based on 97% sequence similarity. The input sequences were processed, and each input sequence was used as a query, then clustered with sequences that had a similarity of 97% or higher. This heuristic approach finds the most similar sequence first, and if no match is found to the sequence being queried, that sequence becomes the centroid of a new cluster (Rognes et al., 2016). The results of OTU clustering is a feature table, which is a matrix that shows the representative sequence from each OTU, as well as an OTU table, which depicts the abundance of each OTU per sample. Afterwards, the obtained OTUs were assigned taxonomy by using the q2-feature-classifier, which is a Naïve Bayesian classifier implemented in QIIME2. The classifier is trained with a database of known rRNA sequences (SILVA rRNA database, containing 2,090,668 16s rRNA sequences) and their taxonomic assignment from domain to genus level. The classifier then divides the sequences into words consisting of 8 base-pairs and counts how many times each word occurred in each taxonomic group. Then, assuming independent probabilities for each word, the classifier uses Bayes' Theorem to calculate the probability that an OTU belongs to each taxonomic group in the training database. After calculating all probabilities, the taxonomic assignment with the highest posterior probability is chosen. The classifier also provides a confidence level for each assignment by taking each OTU representative sequence, dividing it into eight subsequences and attempting classification with this truncated sequence. This gives a bootstrap support value for each taxonomic assignment.

Statistical Analysis. Comparisons between mined and non-mined sites for physical, chemical, and habitat characteristics were made using the Mann-Whitney *U*-test for independent samples. Additionally, comparisons between mined and non-mined sites for elemental analysis (Au, As, S, Hg and MeHg) were made using the Mann-Whitney *U* test. Microbiome comparisons between mined and non-mined sites for phyla, families, and genera were made using the Kruskal Wallis test. Additionally, comparisons between the microbiomes at mined and non-mined sites were performed using the PERMANOVA test. The statistical program (Past3) and QIIME2 were used for calculations.

CHAPTER III

Results and Discussion

Differences in physical, chemical, and habitat characteristics

Physical characteristics. Analysis of measured physical characteristics of water samples revealed a significant difference between certain physical parameters between mined and non-mined sites. The averages of temperature, concentration of total dissolved solids (TDS), and turbidity for all mined sites and all non-mined sites are shown in Figure 8 panel A, and the averages of temperature, concentration of total dissolved solids, and turbidity for the selected sites are shown in Figure 8 panel B, respectively. The temperature, turbidity, and concentration of total dissolved solids for all sites ranged from 27.1°C to 33°C, 11.5 to 111 nephelometric turbidity units (NTU), and 2.39 mg/L to 9.57 mg/L respectively. The temperature between all mined and all non-mined sites differed significantly ($p < 0.01$, Mann-Whitney U test), with significantly higher temperatures at mined sites. The turbidity between all mined and all non-mined sites differed significantly ($p < 0.05$, Mann-Whitney U test), with significantly higher turbidity levels at all mined sites. The concentration of total dissolved solids between all mined and all non-mined sites differed significantly ($p < 0.05$, Mann-Whitney U test), with significantly higher concentrations of total dissolved solids at non-mined sites. It is expected the small sample size ($n=15$) influenced the statistical testing of the selected sites. Although the temperature of the water was determined to be significantly higher at mined sites, temperature of water can be affected by a range of factors including time of day and day itself, vegetation cover, and altitude, thus making this characteristic an unreliable indicator of mining activities. Yet, the observation of higher temperature at mined sites is

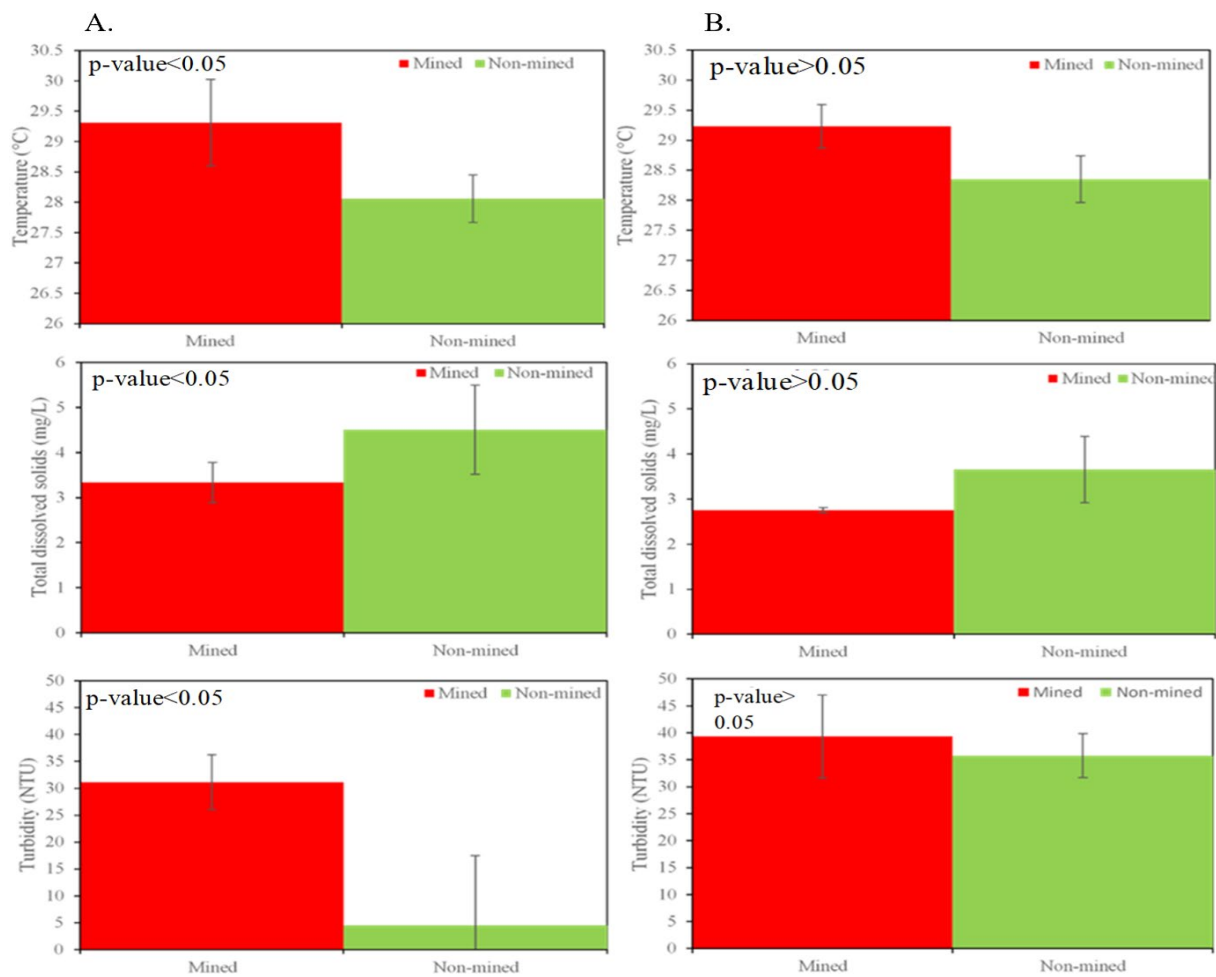


Figure 8. Physical parameters that were significant at sampling sites (red= mined sites, green = non-mined sites). Figure 8A. Average (\pm SD) temperature, total dissolved solids, and turbidity measurements for 17 mined and 10 non-mined sites ($n=81$). Figure 8B. Average (\pm SD) temperature, total dissolved solids, and turbidity measurements for three selected mined and two non-mined sites ($n=15$). Significant differences ($p < 0.05$) were denoted by the p-value in the upper left corner.

still important because higher temperatures have been associated with increased bacterial mercury methylation rates (Ding et al., 2018).

Unlike temperature, turbidity is a promising indicator of mining status. Higher turbidity has been documented at mined sites and historically mined sites by other studies (Gray et al., 2002; Dedieu et al., 2014) and our turbidity data corroborates these findings. Gold mining has been just as strongly associated with increased turbidity as it has been with the release of heavy metals (Hammond et al., 2007; Yule et al., 2010). In addition to releasing heavy metals and increasing turbidity, mining, and especially hydraulic mining, releases massive loads of sediments into the water, and thus increases TDS (Rakotondrabe, et al., 2018). It is important to note that the Guiana shield is characterized by some of the lowest natural suspended solids recorded, and thus any increases in turbidity from mining activities has profound effects (Hammond et al., 2007). For example, past studies indicate turbidity affects stream productivity and species interactions (Parkill & Gulliver, 2002; Izagirre et al., 2009). However, our results showed higher TDS at non-mined sites. The higher concentrations of TDS at non-mined sites could be associated to the geological formation and geomorphology of the location of the non-mined sites, which were situated mostly in tributaries that have headwaters in high elevations which can carry high suspended solids when moving down into the Mazaruni River. It should also be noted that temperature, turbidity, and TDS also can change seasonally (Battin, 1998). Streamflow regime can also control key parameters, including but not limited to, temperature, along the four dimensions of river systems: upstream-downstream, channel-hyporheic, channel-floodplain, and the temporal dimension (Ward, 1989; Amoros & Roux, 1998). In summary, temperature cannot be considered as an

indicator of mining activity, whereas elevated turbidity and increased total dissolved solids have been repeatedly associated with mining activities by other studies. The results for all physical parameters for the 27 sites are given in Appendix C and the results for all physical parameters for the five selected sites are given in Appendix D.

Chemical characteristics. Analysis of measured chemical characteristics of water samples revealed a significant difference between certain chemical parameters between mined and non-mined sites. The averages of electrical conductivity (EC), and pH level for all mined sites and all non-mined sites are shown in Figure 9 panel A, and the averages of electrical conductivity, and pH level for the selected sites are shown in Figure 9 panel B, respectively. The electrical conductivity between all mined and all non-mined sites differed significantly ($p < 0.05$, Mann-Whitney U test), with significantly higher measures of electrical conductivity at non-mined sites. The pH between all mined and all non-mined sites differed significantly ($p < 0.01$, Mann-Whitney U test), with significantly higher pH levels at mined sites. Electrical conductivity and pH did not differ significantly between selected mined and non-mined sites, possibly due to statistical error caused by small sample size.

Electrical conductivity measures the electrical conductance of water and approximates the measure of total dissolved ions salts (Allan & Castillo, 2007). One study that examined the geochemical properties of soil and water around the largest gold mine in Cote d'Ivoire, Africa found that the highest electrical conductivity was in samples collected near tailing storage facilities around the mined sites (Sako et al., 2018). Another study, conducted in Poland, found that streams affected by gold mining activities had the highest electrical conductivity, and the unaffected springs had the lowest

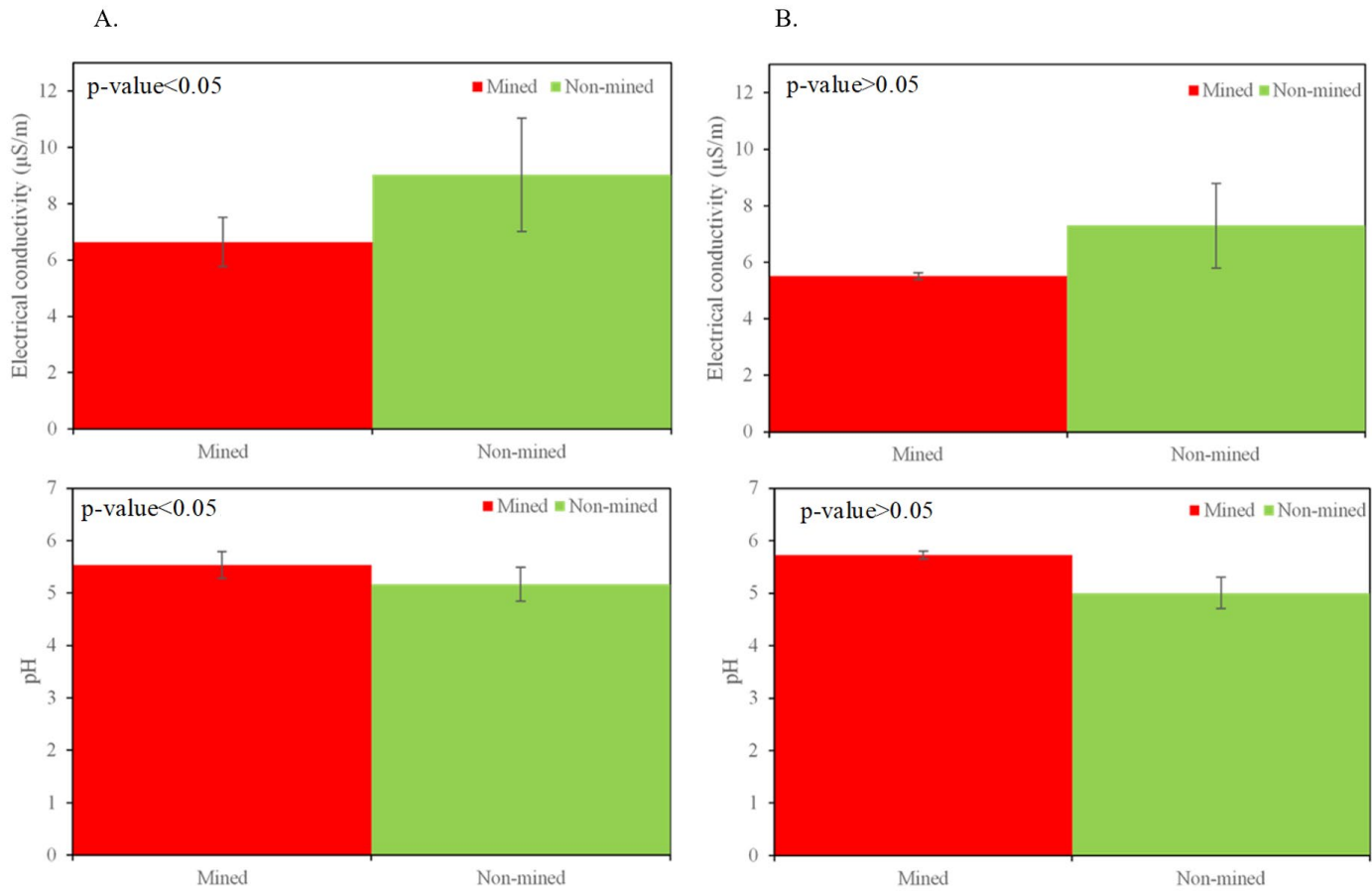


Figure 9. Chemical parameters that were significant at sampling sites (red = mined sites, green = non-mined sites). Figure 9A. Average (\pm SD) electrical conductance and pH for 17 mined and 10 non-mined sites ($n=81$). Figure 9B. Average (\pm SD) electrical conductivity and pH for three selected mined and two non-mined sites ($n=15$). Significant differences ($p<0.05$) were denoted by the p-value in the upper left corner.

(Marszalek & Wasik, 2000). However, our data showed lower EC at mined sites. It is possible this could be due to the geology of the site itself because this determines what minerals are dissolved into the lotic system and thus affects electrical conductivity (Borner et al., 1993). In addition to the geology of the site, weather patterns also affect the EC of river systems. For example, a study was conducted in the Iberian Pyrite Belt which is a place that experiences conditions like Guyana in that there are dry and rainy seasons and gold mining activities there are also polluting river systems with mercury. In that study, it was observed that EC was higher in the dry season as opposed to the wet season, and this was true of all sampling sites regardless of presence or absence of mining activities (Sarmiento et al., 2012). It should be noted that the collection of the sediment samples for this study took place during the dry season in Guyana. If there is high mineral dissolution, higher conductivity will be exhibited. This could be a potential explanation as to why non-mined sites exhibited significantly higher electrical conductivity than did mined sites. Perhaps with further studies that sample over seasons and day and night cycles, the electrical conductivity could be used as an indicator of mining activity.

Acid mine drainage (AMD) is characterized by low pH (Peppas et al., 2000) and is created by mining activities when sulfide-bearing material is exposed to oxygen and water (Akcil & Koldas, 2006). Thus, lower pH was expected to be observed at mined sites. Although our results show lower pH at non-mined sites, this is likely due to the blackwater characteristics of the Mazaruni River. Blackwater rivers are typically tea-colored or black due to high concentrations of dissolved organic matter and are acidic (Duncan & Fernandes, 2010). Thus, the acidic pH found at non-mined sites may just

reflect blackwater properties. Additionally, a similar study to ours which examined mercury content and other physiochemical properties of sediment samples derived from rivers in Guyana, found that the average pH values for mining areas was 6.6 ± 1.1 pH units and ranged from 3.0-7.3 pH units (Howard et al., 2010). The average pH for our mined areas was close but slightly more acidic than this with a pH of 5.54 ± 0.51 . Although our results did not support using pH as an indicator of mining activity, pH is still an important characteristic to note because of its possible effects on mercury uptake by bacteria and thus methylation rates. Kelly et al. 2003 found that increasing the hydrogen ion (H^+) concentration caused large increases in mercury uptake by aquatic bacteria (Kelly et al., 2003). The results for all chemical parameters for the 27 sites are given in Appendix C and the results for all chemical parameters for the five selected sites are given in Appendix D.

Habitat characteristics. Habitat characteristics at sampling sites revealed a significant difference between the mined sites and non-mined sites. The average percentages of macrophytes for all mined sites and all non-mined sites are shown in Figure 10 panel A, and the average percentages of macrophytes for the selected sites are shown in Figure 10 panel B, respectively. The percentage of macrophytes between all mined and non-mined sites differed significantly ($p < 0.01$, Mann-Whitney U test), with a significantly higher percentage of macrophytes present at non-mined sites. Dedieu et al., 2015 assessed the impact of gold mining on biological factors of streams in the Amazon and demonstrated that gold mined sites had more silt and less macrophytes than did non-mined streams. This corroborates our finding that there is a significantly lower percentage of macrophytes at gold mined sites than non-mined. However, there are other

natural factors that may affect macrophyte growth, such as light, sediment type and texture, herbivory and flow rate of the stream (Allan & Castillo, 2007). Because of these reasons and because percentage of macrophytes generally can vary tremendously among

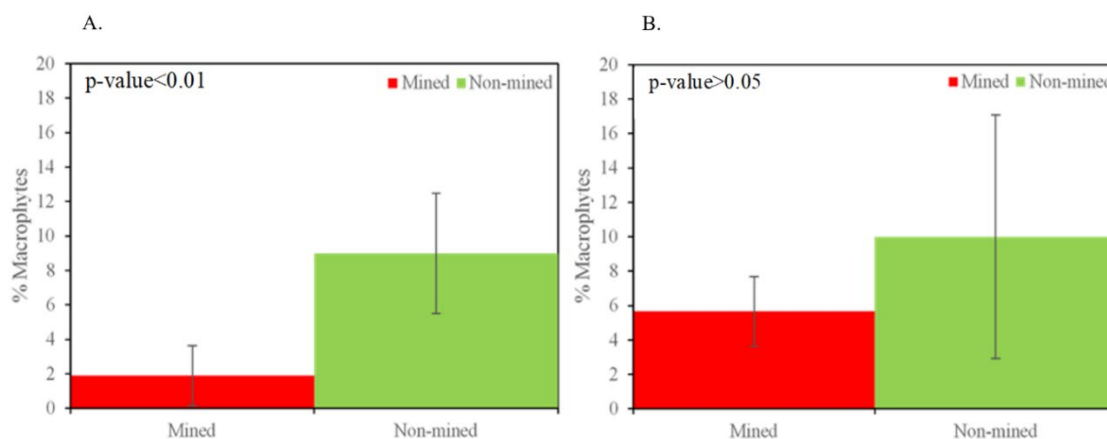


Figure 10. Habitat parameter that was significant at sampling sites (red=mined sites, green=non-mined sites). Figure 10A. Average (\pm SD) percentage macrophytes for 17 mined and 10 non-mined sites. Figure 10B. Average (\pm SD) percentage macrophytes for three selected mined and two non-mined sites. Significant differences ($p < 0.05$) were denoted by the p-value in the upper left corner.

sites, thus smaller percentages of macrophytes should not be considered a reliable indicator of mining activity. The results for all habitat parameters for the 27 sites are given in Appendix C and the results for all habitat parameters for the five selected sites are given in Appendix D.

Elemental analysis

Elemental analysis of Au, As, and S. Chemical analysis indicated a significant variation in the gold, and arsenic, concentrations in the river sediments. The average gold (Au), arsenic (As), and sulfur (S) concentrations for all mined sites and all non-mined sites are shown in Figure 11A and the average concentrations for selected sites are shown in Figure 11B, respectively. The total elemental concentrations for all sites ranged from 0

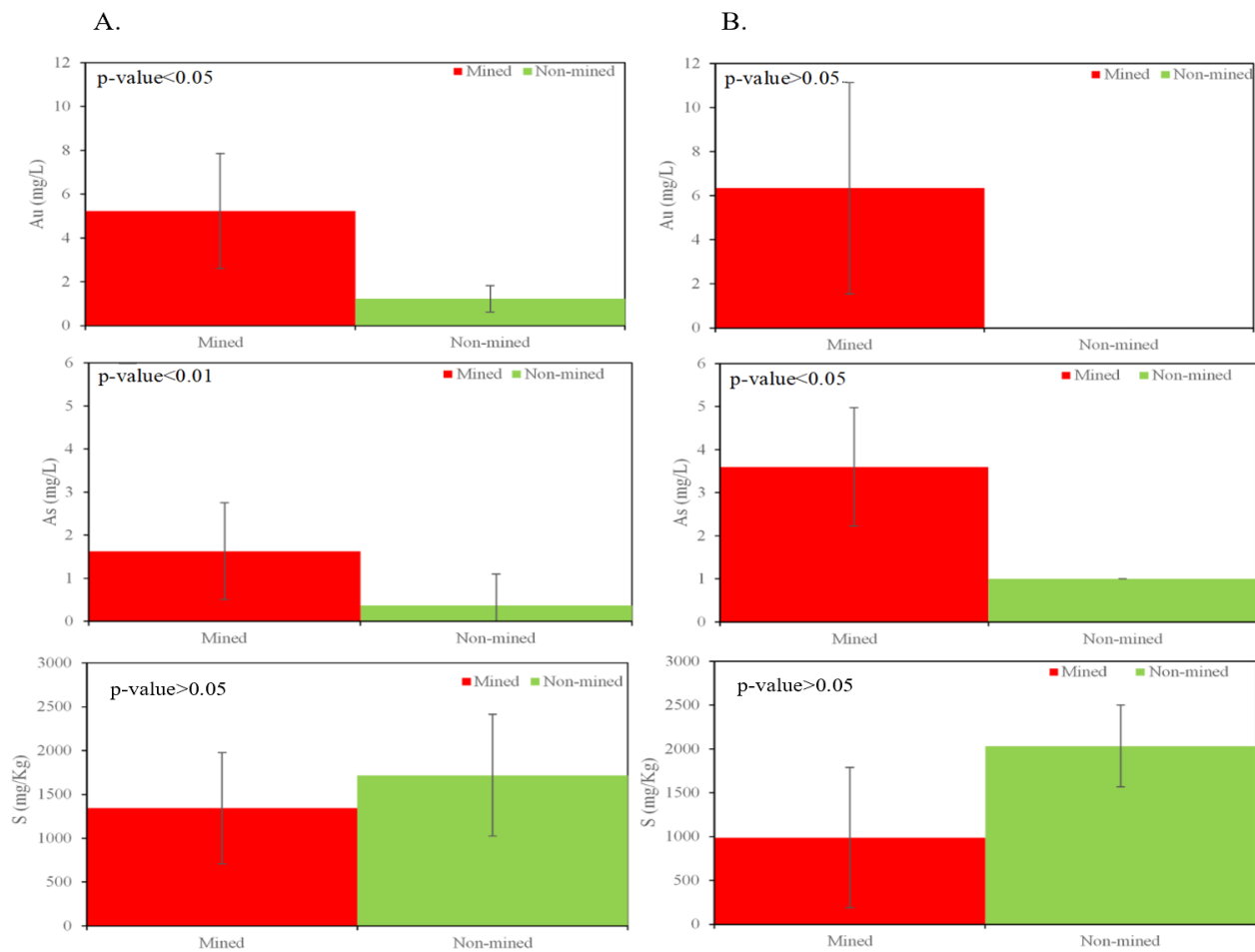


Figure 11. Concentrations of elemental analysis performed in fluvial sediments (red=mined sites, green=non-mined sites). Figure 11A. Average (\pm SD) gold (Au), arsenic (As), and sulfur (S) concentrations for 17 mined and 10 non-mined sites ($n=81$). Figure 11B. Average (\pm SD) gold (Au), arsenic (As), and sulfur (S) concentrations for three selected mined and two non-mined sites ($n=15$). Significant differences ($p<0.05$) were denoted by the p-value in the upper left corner.

to 20.26 mg/L for gold, 0 to 7.98 mg/L for arsenic, and 0 to 5851.94 mg/Kg for sulfur. The average elemental concentrations for all mined sites were 5.23 ± 7.18 mg/L for Au, 1.63 ± 2.25 mg/L for As, and 1345.10 ± 1266.29 mg/Kg for S. The average elemental concentrations for non-mined sites were 1.22 ± 2.51 mg/L for Au, 0.37 ± 1.47 mg/L for As, and 1719.35 ± 1386.98 mg/Kg for S. Au concentrations between all mined and all non-mined sites had a highly significant difference ($p < 0.01$, Mann-Whitney U test), with Au concentrations being significantly higher at mined sites. The concentrations of Au were always higher at mined sites than at non-mined sites except for non-mined sites 18 and 21 which demonstrated average Au of 5.79 mg/L and 6.43 mg/L, respectively. As concentrations among all mined and all non-mined sites also had highly significant differences ($p < 0.01$, Mann-Whitney U test), with As concentrations being significantly higher at mined sites. On average, the highest concentrations of As were found in the gold mined areas, notably mined site 33 with 5.76 mg/L. The recommended level of arsenic in water is less than $10\text{-}50\mu\text{g/L}$ (Ratnaike, 2003), placing these concentrations well over advised. The concentrations of S were not significantly different among all mined and all non-mined sites ($p > 0.05$, Mann-Whitney U test). When comparing the concentrations of Au for selected mined sites against selected non-mined sites, selected mined sites had higher concentrations of Au, whereas at selected non-mined sites the Au concentrations were non-detectable. The concentrations of As for selected mined sites were significantly higher than non-mined sites ($p < 0.05$, Mann-Whitney U test). The concentrations of S for selected sites was significantly different between mined and non-mined sites ($p < 0.05$, Mann-Whitney U test), with higher S concentrations at non-mined sites. In summary, the mined sites exhibited higher concentrations of Au and As in the

sediment samples than the non-mined sites. This data supports our hypothesis that there would be significantly different elemental concentrations between mined and non-mined sites.

Guyana is endowed with major Au deposits and the higher concentrations of Au exhibited at mined sites was expected (Bertoni et al., 1991). The occurrence of higher Au concentrations at mined sites is likely due to the lithostratigraphic characteristics and not due to the mining activities themselves. Gold deposits and occurrences across the Guiana Shield are associated with low- to medium metamorphic-grade granitoid-greenstone belts and are often located near quartz veins (Kerrich and Cassidy, 1994; Milesi et al., 1995).

It was suspected that higher levels of As would be exhibited at the mined sites due to the propensity of mining processes to release arsenic. This occurs because As is naturally associated with pyrite (FeS) and arsenopyrite (FeSAs₂), and gold mining activities favor As mobilization (Kesse, 1985). In addition to releasing As, gold mine tailings have also been known to contain many sulfide minerals, which is why an increase of S was expected to be observed at mined sites (Kiventera et al., 2018). In contrast, when examining all the sites, this data displayed no difference in S concentration between mined and non-mined sites. However, the concentration of S is still of interest due to its ability to affect the availability of mercury. This is because Hg has a high affinity for sulfur-containing ligands, and these sulfur mercury complexes are often more stable than water soluble Hg (Hintelmann et al., 1995). Concentrations of Au, As, and S for all 27 sites are given in Appendix E and concentrations of Au, As, and S for the five selected sites are given in Appendix F.

Elemental analysis of Hg and MeHg. Mercury (Hg) concentrations varied significantly in the river sediments. The average mercury concentrations for all sites and selected sites are shown in Figure 12A and Figure 12B, respectively. The total Hg concentrations for all mined sites ranged from 0 to 18.065 $\mu\text{g}/\text{Kg}$, and 0 to 6.805 $\mu\text{g}/\text{Kg}$ for all non-mined sites. The average Hg concentrations for all mined sites were $2.102 \pm 3.983 \mu\text{g}/\text{Kg}$ and $0.774 \pm 1.749 \mu\text{g}/\text{Kg}$ for all non-mined sites. Hg concentrations varied significantly between all mined and all non-mined sites ($p < 0.001$, Mann-Whitney U test), with mined sites having higher concentrations. Two non-mined sites (2 and 11), registered average Hg concentrations of 5.211 $\mu\text{g}/\text{Kg}$ and 2.743 $\mu\text{g}/\text{Kg}$, respectively. Concentrations of Hg for selected sites showed repeatedly higher concentrations of Hg for mined sites when compared to non-mined sites. The average concentration of Hg for selected mined sites was $8.613 \pm 5.972 \mu\text{g}/\text{Kg}$ versus $0.039 \pm 0.061 \mu\text{g}/\text{Kg}$ for non-mined sites. The concentrations of Hg for selected mined sites were significantly higher than non-mined sites ($p < 0.001$, Mann-Whitney U test). When comparing the Hg contamination levels of the main channel of the Mazaruni River to that of two of its tributaries sampled from, the Kurupung and the Eping, the Mazaruni River channel registered the highest concentrations of Hg (average $2.77 \mu\text{g}/\text{Kg} \pm 4.58$); while the Kurupung, part of which is affected by mining activities, had on average 0.16 $\mu\text{g Hg}/\text{Kg}$ (± 1.58). The Eping, a relatively less impacted tributary, had an average of 0.04 $\mu\text{g Hg}/\text{Kg}$ (± 0.06), making it the least contaminated tributary by gold mining activities. Selected samples were analyzed for MeHg using gas chromatography cold vapor atomic fluorescence spectroscopy (GC-CVAFS). The concentration of MeHg ranged from 0.03 to 2.16 $\mu\text{g Hg}/\text{Kg}$ at mined sites, and from 0 to 0.055 $\mu\text{g Hg}/\text{Kg}$ at non-mined sites. The

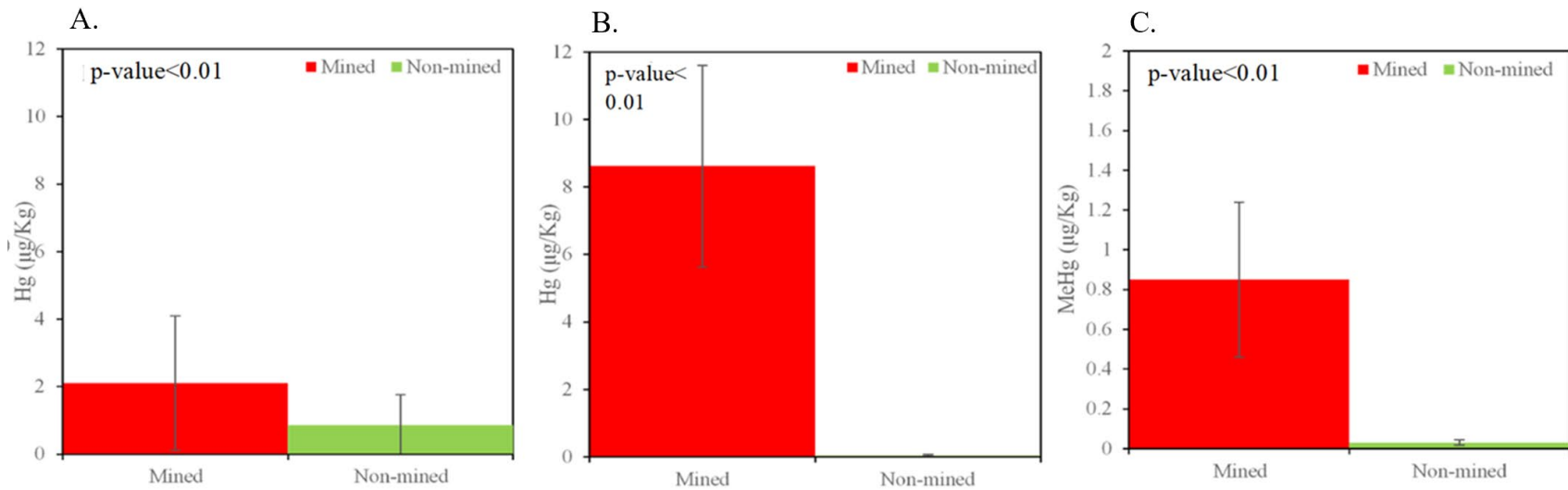


Figure 12. Total mercury concentrations in the study sites (red = mined sites, green = non-mined sites). Figure 12A. Average (\pm SD) total mercury (Hg) concentrations for 17 mined and 10 non-mined sites (n=81). Figure 12B. Average (\pm SD) total mercury (Hg) concentrations for three selected mined and two non-mined sites (n=15). Figure 12C. Average (\pm SD) methyl mercury (MeHg) concentrations for three selected mined and two non-mined sites (n=15). Significant differences ($p < 0.05$) were denoted by the p-value in the upper left corner.

average MeHg concentration at mined sites was $0.85 \pm 0.80 \mu\text{g Hg/Kg}$ and $0.03 \pm 0.03 \mu\text{g Hg/Kg}$ at non-mined sites. The average MeHg concentrations for selected mined sites and non-mined sites are shown in Figure 12C. MeHg was significantly higher at mined sites than at non-mined sites ($p < 0.01$, Mann-Whitney U test). Average Hg and MeHg concentrations for selected sites mined and non-mined are shown in Figure 13A, and Figure 13B, respectively. Figure 13C displays the average Hg and MeHg concentrations at non-mined sites on a 100 magnitude lower scale than the previous figures to better visualize the small-scale differences between Hg and MeHg concentrations. Including MeHg data from both mined and non-mined sites, MeHg accounted for 10.05% of the total Hg (THg) present. Interestingly, MeHg accounted for 9.87% of total Hg at mined sites and for 68.82% at non-mined sites. Our hypothesis that higher concentrations of Hg and MeHg would exist at mined sites was supported with the result. Although a past study conducted on the Mazaruni River recorded higher mercury levels in the channel bed sediments (average Hg concentrations of $0.077 \mu\text{g g}^{-1}$) (Miller et al., 2003), our results still, even with the smaller concentration of Hg, indicate significantly higher Hg concentration at mined sites as opposed to non-mined sites. Higher concentrations of Hg allow for greater methylation, and thus the significantly higher MeHg concentration at mined sites was expected and observed. Concentrations of MeHg for the five selected sediment samples are given in Appendix G and the average concentrations of Hg, MeHg, Au, As, and S and their p-values are provided in Appendix H.

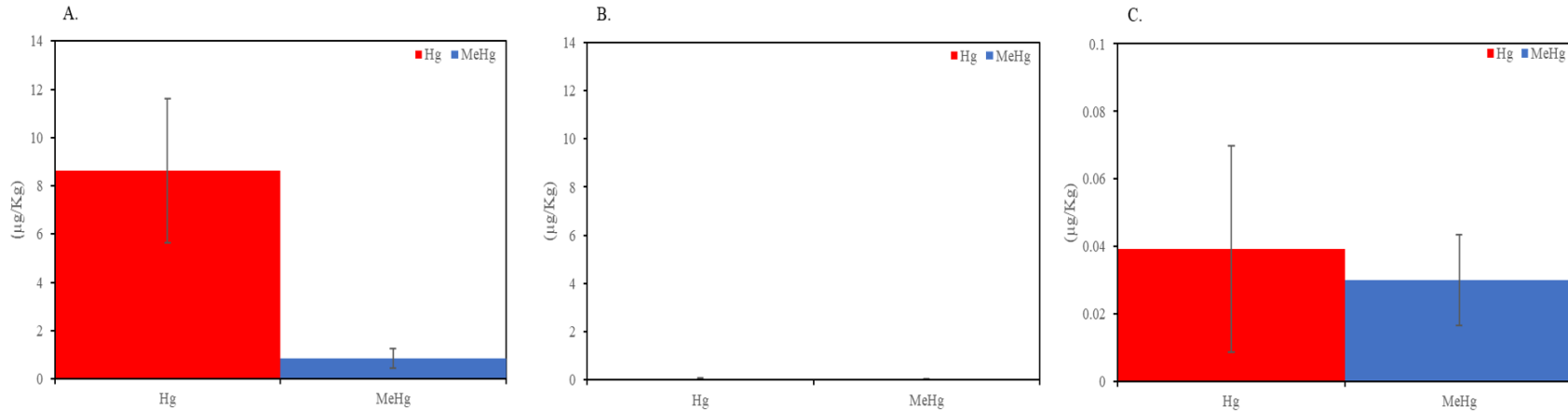


Figure 13. Comparison of average mercury (red) and methyl mercury (blue) concentrations. Figure 13A. Average (\pm SD) mercury (Hg) and methyl mercury (MeHg) concentrations for three selected mined sites (n=9). Figure 13B. Average (\pm SD) mercury (Hg) and methyl mercury (MeHg) concentrations for two selected non-mined sites (n=6). Figure 13C. Average (\pm SD) mercury (Hg) and (MeHg) concentrations for selected non-mined sites exhibited at 100 magnitude lower scale.

Microbiome analysis

Length distribution, rarefaction curve of alpha diversity, principal coordinate analysis, and OTU distribution. A total of 310,302 16S rDNA sequences were available for microbiome analysis. On average, each sample provided 20,686 (SD \pm 5947) sequences. The distribution of these sequence lengths is shown in Figure 14.

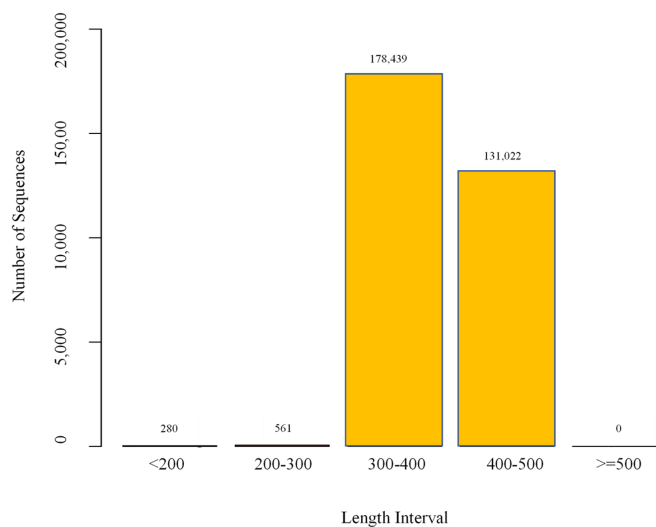


Figure 14. Length distribution of 16S rDNA sequences.

All sequences were of 300-500 nucleotides in length which are within the expected range of amplicon sizes of 16S rRNA genes across bacterial species. Of the total sequences, 178,439 sequences (57.5%) were of 300-400 nucleotide lengths, while 131,022 sequences (42.2%) were of 400-500 nucleotide lengths. Although sequence length of 16S rRNA gene varies, overall GC composition of these sequences remains ~55-57%.

Rarefaction curve analysis, which measured number of observed OTUs against increasing sequence depth for each replicate is shown in Figure 15. Result shows that mined site 33 replicate B exhibited the highest diversity (Shannon index=8.84) and mined

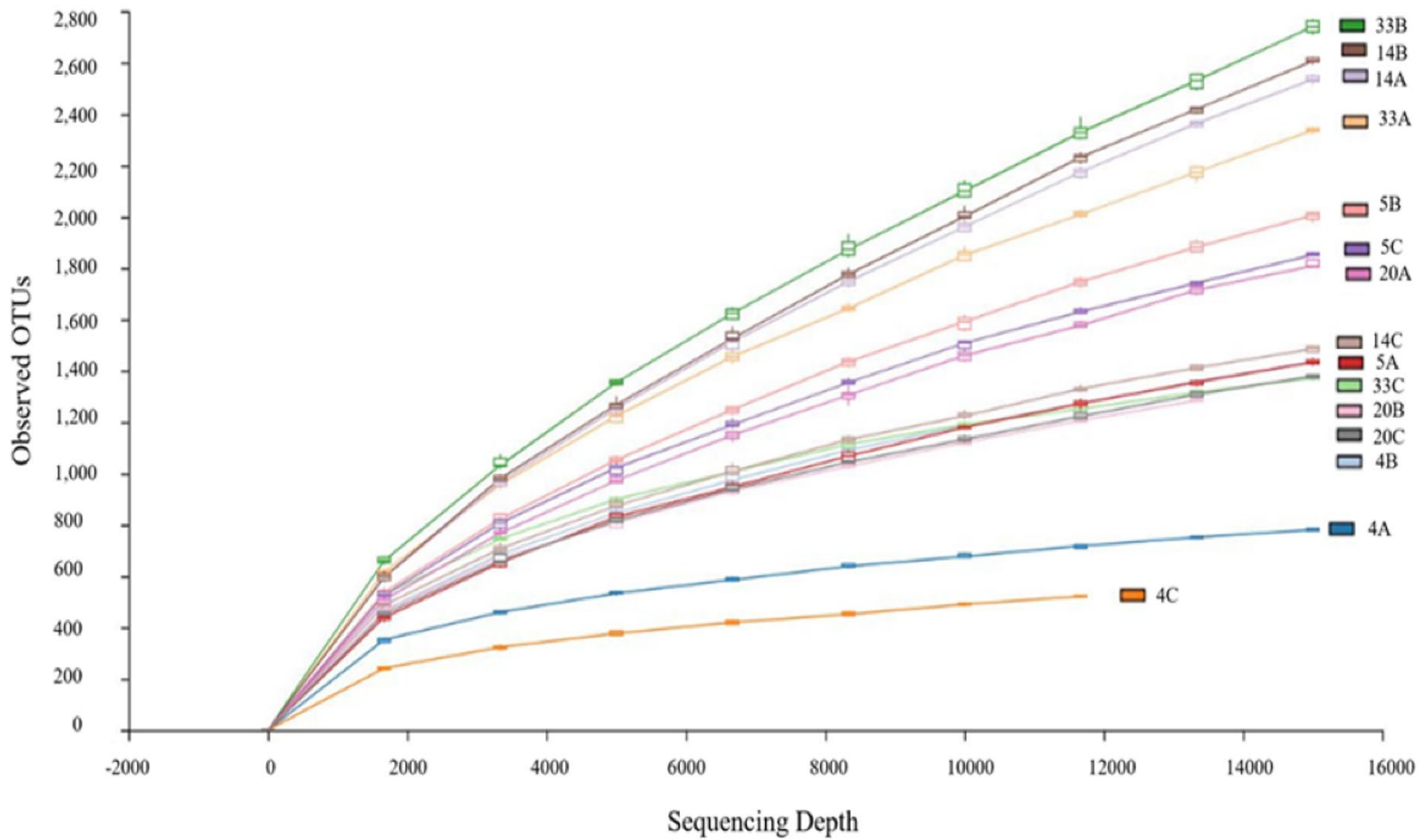


Figure 15. Rarefaction curve of alpha diversity in fluvial sediment samples collected in triplicates from three mined and two non-mined sites (n=15).

site 4 replicate C exhibited the lowest diversity (Shannon index=6.24). At all these sites, increase in the rate of randomly collected OTUs starts to slow down after increasing the number of randomly selected sequence tags. This suggests that even if we collected more sequences there would be no significant increase in total numbers of unique OTUs from these samples. Furthermore, the alpha diversity within each site is shown in Figure 16. Mined site 4 had the lowest number of observed OTUs while mined site 33 and non-mined site 14 showed the highest number of observed OTUs.

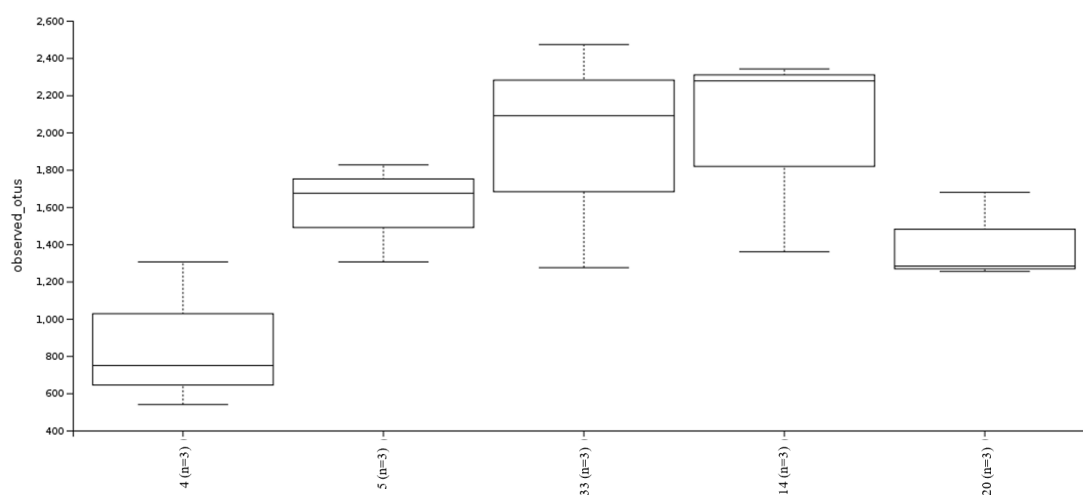


Figure 16. Box plots of observed OTUs for three mined and two non-mined sites. The median value is shown as a *line* within the box. Whiskers extend to the most extreme values.

Figure 17 exhibits the principal coordinate analysis (PCoA) of weighted UniFrac phylogenetic distances based on shared and unshared OTU sequences within replicate pairs within each mined and non-mined site and between all possible pairs within mined and non-mined sites. The phylogenetic distances reflect upon the differences in the community structure within and between these sites. Results as shown in Figure 17 suggest that the OTU composition across these sites are clustered into groups,

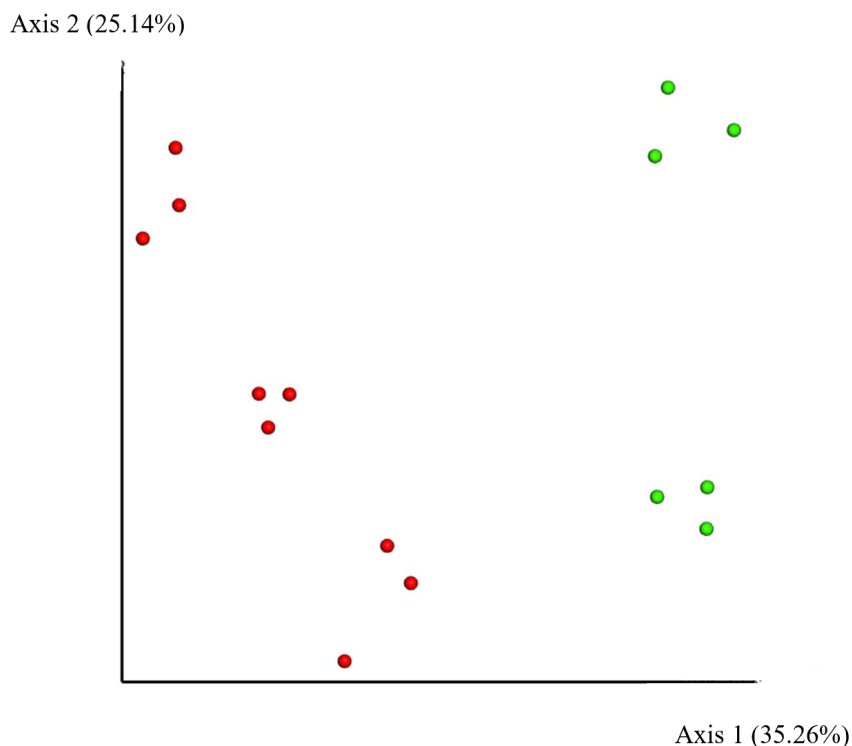


Figure 17. Principal coordinate analysis (PCoA) plot of the weighted UniFrac distances at three mined (red) and two non-mined (green) sites.

mined (red) and non-mined (green) sites. In addition, the dissimilarity of the OTU composition across mined and non-mined sites are also separated into distinct clusters for mined and non-mined sites. Together, the two axes, as shown in Figure 17 accounted for 60.4% variation in OTU composition. Furthermore, the bacterial community structure at mined sites was significantly different from non-mined sites (PERMANOVA analysis: $F = 1.8186$, $p = 0.002$). A total of 15,681 OTUs were identified, of which, 1,536 OTUs were classified in the domain of Bacteria, 12 in Archaea, and 1 remained unclassified. Of the total OTUs, 15,535 were assigned to known bacterial phyla. Figure 18 displays the number of OTUs that were shared by and unique to the mined and non-mined sites. Of the total OTUs, 7,419 OTUs were unique to mined sites, 5,648 OTUs were unique to non-mined sites, and 2,614 OTUs were shared by mined and non-mined sites.

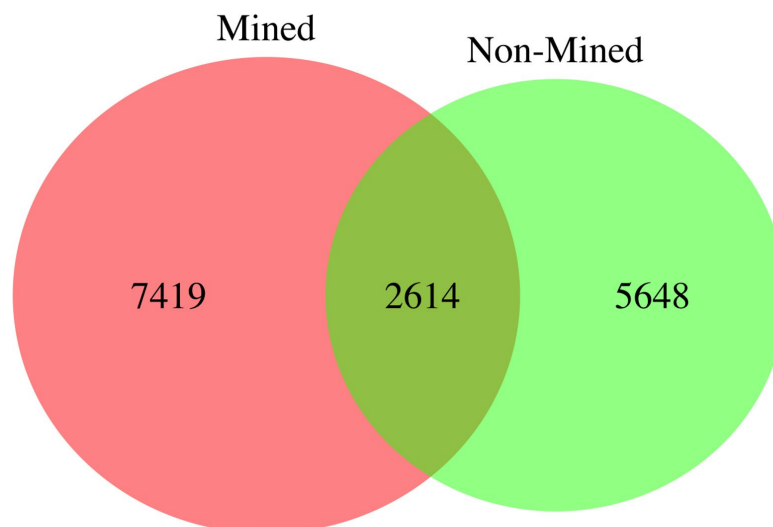


Figure 18. Venn diagram of unique and shared OTUs found at mined and non-mined sites.

Distribution of bacterial phyla abundance. Soil sediments of rivers are complex ecological niches that are the outcome of the accumulation of organic matter and are inhabited by a variety of eukaryotic and prokaryotic microorganisms. The structure of the sediment microbial community is affected by physiochemical characteristics of the sediment and by the loads of organic matters and anthropogenic toxic pollutants introduced to the aquatic system (Acosta-Martinez et al., 2008). Additionally, the bacterial community composition of rivers is also shaped by water temperature, day length, time, water residency duration, pH (Niño-García et al., 2016), available nutrients (Ruiz-Gonzalez et al., 2015), and storm events (Jackson et al., 2014). Thus, the nature of the sediment microbiome of the Mazaruni River is complex and multivariable. However, because mined-sites were contaminated with mercury and other mining related effluents, it was hypothesized that the microbial community structure and composition would be significantly different between mined and non-mined sites. The

bacterial diversity for most prevalent phyla at mined and non-mined sites is depicted in Figure 19 and the phyla determined to be significant (p -value <0.05) are shown in Table 1. The average percent abundance and Kruskal Wallis test results for each phylum (significant and non-significant) can be found in Appendix I. A majority of the OTUs (~82%) represent two major phyla, *Proteobacteria* and *Actinobacteria* at both mined and non-mined sites. *Proteobacteria* was found more abundant Kruskal Wallis test, ($p < 0.01$) at mined sites (46.23%) than the non-mined sites (34.23%), while *Actinobacteria* were found more abundant (Kruskal Wallis test, $p < 0.01$) at non-mined sites (34.39%) than the mined sites (25.78%). Although *Elusimicrobia* is less abundant at both mined (0.21%) and non-mined (0.6%) sites, members of this phylum are significantly higher (Kruskal Wallis test, $p < 0.01$) at mined sites. Four additional bacterial phyla, unclassified *Bacteria* (*Bacteria*_), *WPS-2*, *Cyanobacteria*, *Planctomycetes*, and *Patescibacteria*, were less abundantly present at both mined and non-mined sites; however, they were significantly higher (Kruskal Wallis test, $p < 0.05$) at non-mined sites. Furthermore, mined and non-mined sites contain 0.16% and 0.39% unclassified phyla, respectively and these additional phyla may represent new taxa which have not been classified yet.

Proteobacteria comprises the largest and most phenotypically diverse phylum of the prokaryotes and is of great biological significance because it includes many known animals and plant pathogens such as *Escherichia*, *Salmonella*, *Vibrio*, and *Helicobacter* (Holt et al., 1994; Gupta, 2000). It is likely that the pervasive presence of *Proteobacteria* is due to the robustness of the members of this phylum to exist in multivariable and complex hostile environmental conditions, such as heavy metal-rich environments (Rastogi et al., 2010). Furthermore, studies conducted on samples derived from Uranium

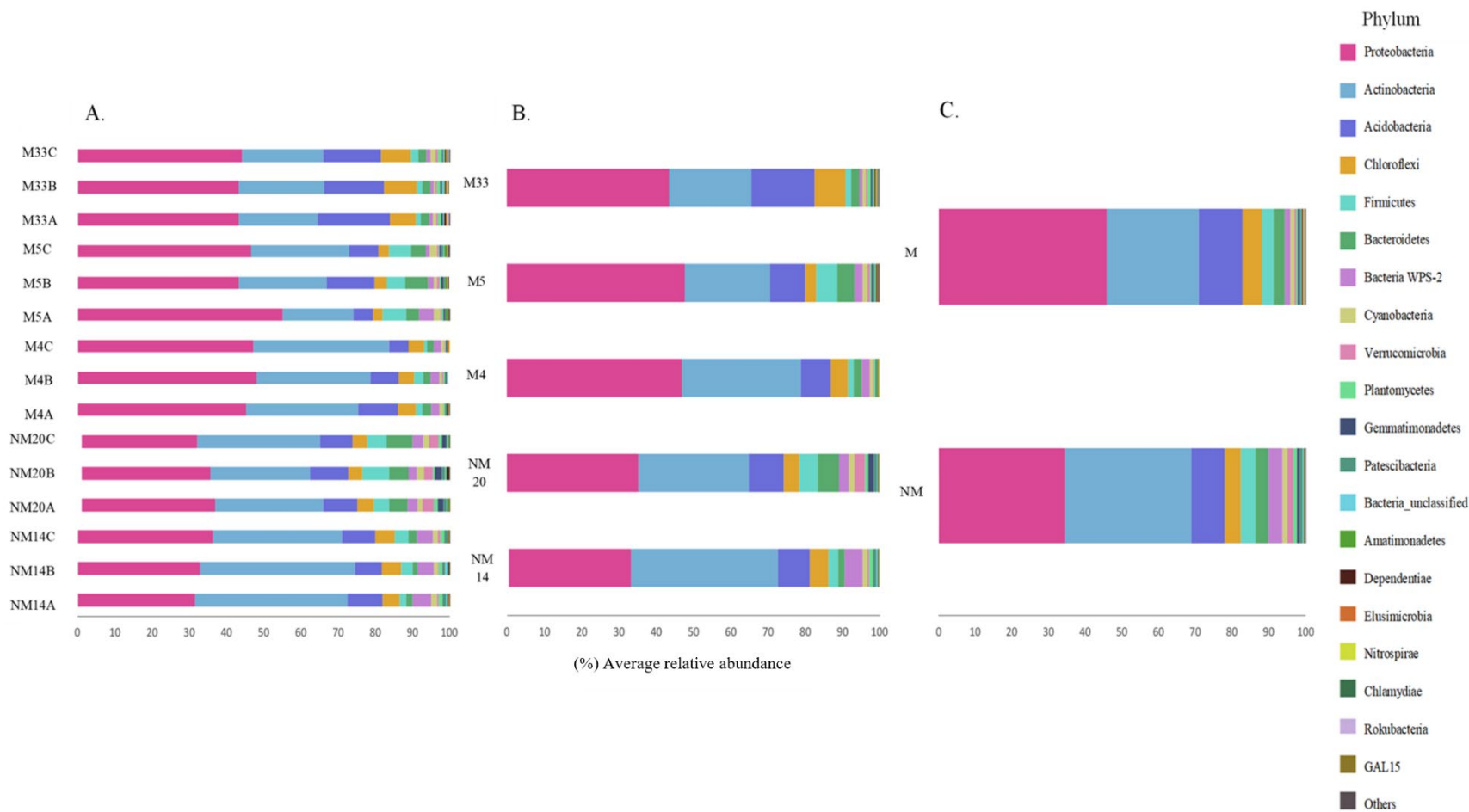


Figure 19. Taxonomic distribution of top 20 most abundant phyla at mined (M) and non-mined (NM) sites. Figure 19A. Relative phyla abundances in three replicates of each mined and non-mined sites (n=15). Figure 19B. Relative phyla abundances of three mined and two non-mined sites. Figure 19C. Relative phyla abundances of the total mined and non-mined sites.

Table 1

Average relative abundance (%) of phyla and results of Kruskal Wallis tests for significantly different phyla ($p < 0.05$) between mined and non-mined sites

Phylum	Average relative abundance (%)		Kruskal Wallis
	Mined	Non-mined	p-value
Actinobacteria	25.78	34.39	0.025
BRC1	0.02	0.00	0.048
Cyanobacteria	1.07	1.50	0.045
Dadabacteria	0.02	0.00	0.035
Elusimicrobia	0.21	0.06	0.003
Patescibacteria	0.36	0.73	0.007
Planctomycetes	0.60	0.96	0.025
Proteobacteria	46.23	34.23	0.001
WPS-2	1.78	3.55	0.007
Bacteria	0.14	0.37	0.018

mined sites in India and Gold mined sites in Africa report similar findings, with *Proteobacteria* being the most abundant phylum in mine tailings and acid mine drainage (Dhal and Sar, 2014; Keshri et al., 2015). Additionally, numerous members of the δ -*Proteobacteria* class are known mercury methylators, and their genomes possess *hgcA* and *hgcB* genes, which are involved in the mercury methylation reactions. Also, a recent study by Macdonald (2016) showed that *Elusimicrobia* existed in waters affected by mine-water discharge. Similarly, Chen et al., (2018) found that the presence of bacterial phyla such as *Actinobacteria* and *Verrucomicrobia* is negatively correlated with high concentration of heavy metals, such as Hg, As, and Pb, suggesting that members of these two phyla may have heavy metal sensitivity. These findings could help to explain why these two phyla were less abundant at non-mined sites in this study, for which our elemental analysis exhibited higher concentrations of Hg and As. Also, within the *Proteobacteria*, γ -proteobacteria was found to be more abundant at mined sites (19.31%) than at non-mined sites (10.03%) (Kruskal Wallis test, p -value <0.01). This result could be due to the heavy metal tolerance

capabilities of γ -proteobacteria, because this group harbors the highest frequency of metal resistance related genes within *Proteobacteria*. The correlation between mercury concentration and γ -proteobacteria abundance is shown in Figure 20. The correlation coefficient was 0.85, indicating mercury concentration and percent average relative abundance of γ -proteobacteria was positively correlated.

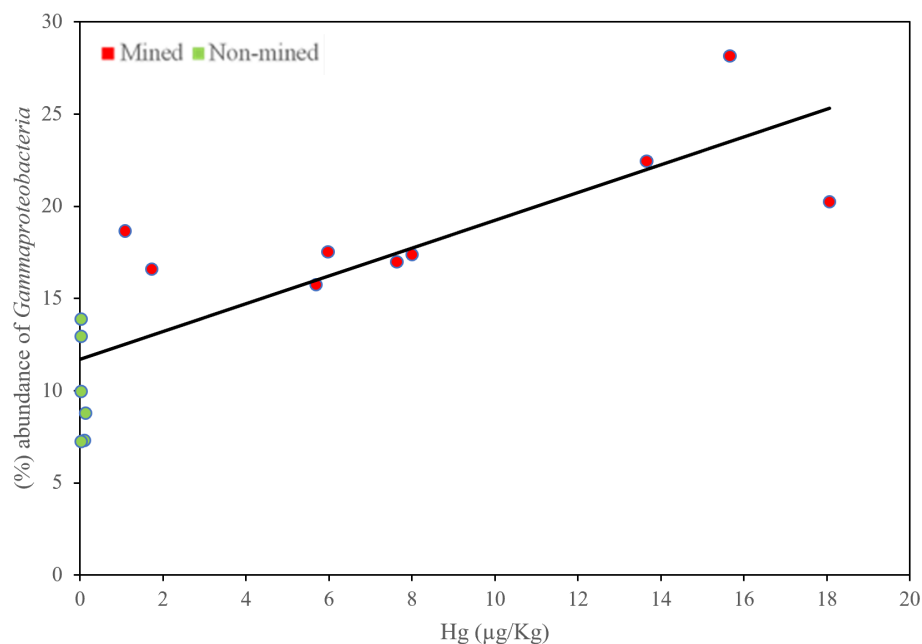


Figure 20. Scatterplot relating mercury (Hg) concentration and percent abundance of γ -proteobacteria. The mined and non-mined sites are indicated in red and green circles, respectively.

Distribution of bacterial family abundance. Bacterial family diversity at mined and non-mined sites is shown in Figure 21 and the families determined to be significant (p -value <0.05) are shown in Table 2. The average abundance and Kruskal Wallis test results for each family (significant and non-significant) can be found in Appendix J. Results reveal the bacterial family *Burkholderiaceae* was the most abundant at both mined and non-mined sites, but it is significantly higher (Kruskal Wallis test, $p < 0.01$) at mined

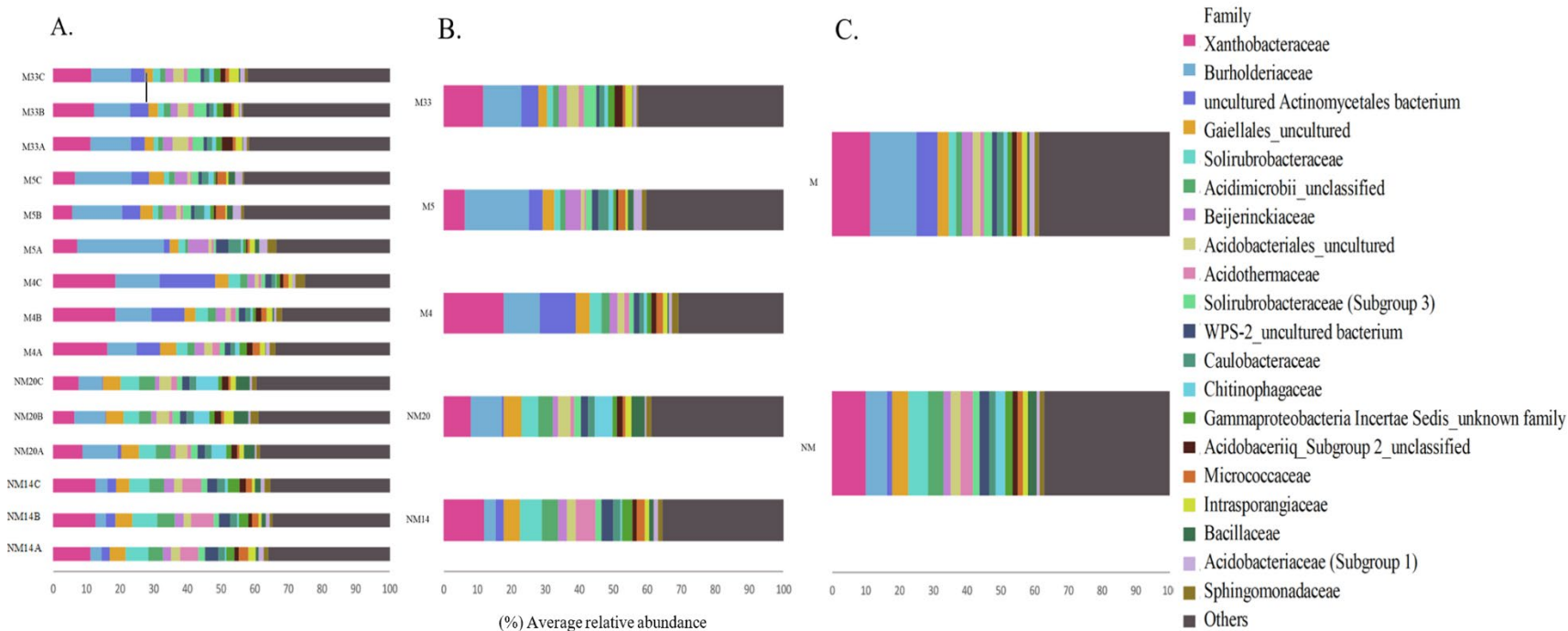


Figure 21. Taxonomic distribution of top 20 most abundant family groups at mined (M) and non-mined (NM) sites. Figure 21A. Relative family abundances in three replicates of each mined and non-mined sites (n=15). Figure 21. Relative family abundances of three mined and two non-mined sites. Figure 21C. Relative family abundances of the total mined and non-mined sites.

Table 2

Average relative abundance (%) of family groups and results of Kruskal Wallis tests for significantly different family groups ($p < 0.05$)

Family	Average relative abundance (%)		Kruskal Wallis p-value
	Mined	Non-mined	
Elsteraceae	0.13	0.00	0.001
Micropepsaceae	0.49	0.78	0.025
Paracaedibacteraceae	0.01	0.05	0.008
KF-JG30-B3	0.38	0.05	0.005
Rhodomicrobiaceae	0.16	0.37	0.005
Magnetospirillaceae	0.32	0.01	0.002
AB1	0.00	0.04	0.001
Desulfobulbaceae	0.08	0.00	0.035
Geobacteraceae	0.94	0.00	0.021
MBNT15_	0.03	0.00	0.017
Haliangiaceae	0.42	0.95	0.005
Polyangiaceae	0.43	0.74	0.01
Sandaracinaceae	0.02	0.00	0.006
0319-6G20	0.61	1.84	0.018
Oligoflexaceae	0.06	0.24	0.002
SAR324 clade (Marine group B)	0.02	0.00	0.035
Syntrophobacteraceae	0.09	0.00	0.013
TX1A-33	0.03	0.00	0.017
Beggiatoaceae	0.45	0.00	0.017
Burkholderiaceae	13.79	6.06	0.003
Ferrovaceae	0.77	0.00	0.007
Gallionellaceae	0.10	0.00	0.017
Nitrosomonadaceae	0.77	0.15	0.013
Rhodocyclaceae	0.26	0.00	0.013
SC-I-84	0.21	0.02	0.003
Betaproteobacteriales_	0.11	0.01	0.007
Coxiellaceae	0.01	0.03	0.007
JG36-TzT-191_	0.20	0.46	0.013
WD260	0.02	0.13	0.001
Rhodanobacteraceae	0.06	0.22	0.003
Uncultured Firmicutes bacterium	0.10	0.34	0.018

sites (13.79%) than non-mined sites (6.06%). The family *Burkholderiaceae* is comprised of genera which are phenotypically, metabolically and ecologically diverse. Members of this family include both strictly aerobic, facultatively anaerobic, chemoorganotrophs, obligate facultative chemolithotrophs, and pathogens (Garrity et al., 2015). Members of this family are also capable of metal and sulfate reduction and are reported to live in association with other sulfur reducing bacteria (SRB) when the environment is affected

by high metal concentrations (Church et al., 2007; Van der Zaan et al., 2012). Uncultured *Actinomycetales* was also found to be significantly more abundant (Kruskal Wallis test, $p < 0.01$) at mined sites (6.66%) than non-mined (1.50%). The order *Actinomycetales* includes generally anaerobic bacteria that contain both free living and pathogenic species, which are considered quintessential degraders of complex polysaccharides in soils (Yeager et al., 2017). In contrast, the family *Solirubrobacteraceae* was significantly more abundant (Kruskal Wallis test, $p < 0.01$) at non-mined sites (5.84%) than mined sites (2.34%). Members of the family *Solirubrobacteraceae* are mesophilic and psychrotolerant (capable of growing at temperatures close to freezing but optimal growth temperature is higher) (Gundlapally et al., 2009).

Distribution of bacterial genera. Bacterial genera diversity at mined and non-mined sites is shown in Figure 22. The predominant genera observed at mined sites were uncultured bacteria of *Actinomycetales* (6.66%), uncultured bacteria of *Xanthobacteraceae* (5.64%), unclassified genera of *Burkholderiaceae* (4.24%), and *Burkholderia-Caballeronia-Paraburkholderia* (4.0%). The predominant genera at non-mined sites included unclassified genus of *Xanthobacteraceae* (5.43%), unclassified *Acidimicrobiia* (4.52%), and uncultured *Gaiellales* (4.27%). Genera *Actinomycetales* (6.66%), *Burkholderia-Caballeronia-Paraburkholderia* (4.23%), uncultured *Burkholderiaceae* (4.24%), *Ramlibacter* (2.28%), and *Pseudolabrys* (2.06%) were found at a significantly higher percentage of composition at mined sites than non-mined sites (Kruskal Wallis test, $p < 0.01$). Genera that were significantly more abundant at non-mined sites included uncultured *Gaiellales* (4.30%), uncultured *Acidimicrobiia* (4.49%),

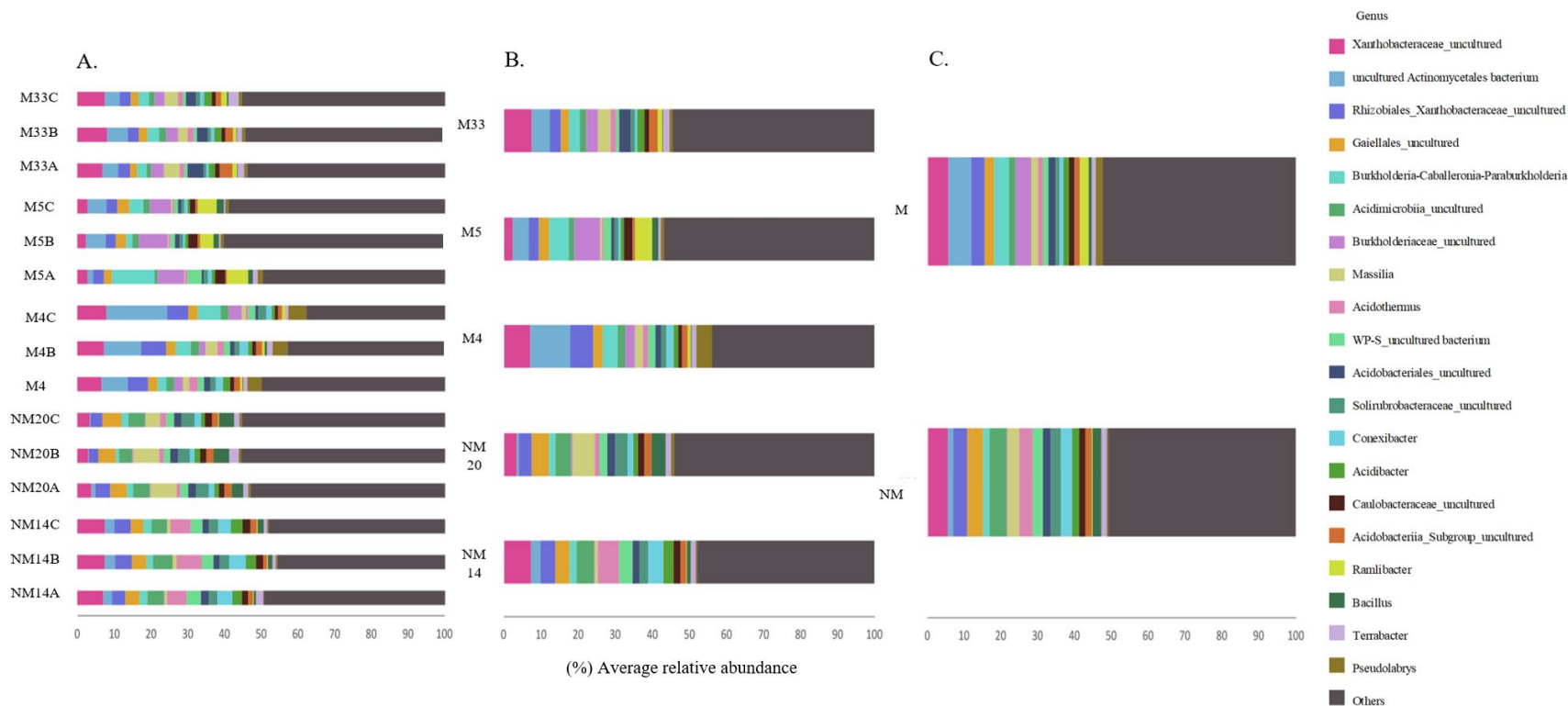


Figure 22. Taxonomic distribution of top 20 most abundant genera at mined (M) and non-mined sites (NM). Figure 22A. Relative genera abundances in three replicates of each mined and non-mined sites (n=15). Figure 22B. Relative genera abundances of three mined and two non-mined sites. Figure 22C. Relative genera abundances of the total mined and non-mined sites.

Table 3

Average relative abundance (%) of top 20 genera and results of Kruskal Wallis test for significantly different genera ($p < 0.05$) with the top 20 genera between mined and non-mined sites

Genus	Average relative abundance (%)		Kruskal Wallis
	Mined	Non-mined	p-value
Uncultured Actinomycetales bacterium	6.66 ± 4.36	1.50 ± 1.20	0.004
Burkholderiaceae_uncultured	4.24 ± 2.15	0.22 ± 0.09	0.001
Burkholderia-Caballeronia-Paraburkholderia	2.34 ± 3.03	1.72 ± 0.50	0.007
Ramlibacter	2.28 ± 2.05	0.17 ± 0.03	0.001
Pseudolabrys	2.06 ± 1.68	0.58 ± 0.18	0.003
Acidimicrobiia_uncultured	1.77 ± 0.44	4.49 ± 0.58	0.001
Gaiellales_uncultured	2.47 ± 0.44	4.30 ± 0.60	0.001
Solirubrobacteraceae_uncultured	1.16 ± 0.38	2.94 ± 0.53	0.001
Conexibacter	1.16 ± 0.62	2.77 ± 1.43	0.018
WPS-2_uncultured bacterium	1.60 ± 0.94	2.74 ± 0.77	0.018
Bacillus	0.72 ± 0.67	2.57 ± 1.50	0.010

uncultured WPS-2 bacterium (2.74%), uncultured *Solirubrobacteraceae* (2.94%), *Conexibacter* (2.77%), and *Bacillus* (2.57%). The genus *Burkholderia-Caballeronia-Paraburkholderia* is a relatively new genus (Estrada-de los Santos, 2018). The species belonging to the genus *Burkholderia* exhibit various lifestyles including human, animal, and plant pathogens, strains with significant biotechnological potential, and plant symbionts (Depoorter et al., 2016; Suarez-Moreno et al., 2012, Beukes et al., 2017). *Ramlibacter* are aerobic, chemo-organotrophic, and cyst-producing soil bacteria (Heulin et al., 2003).

Distribution and diversity of known mercury methylators at mined and non-mined sites. The main mechanism for Hg methylation within various ecosystems is mediated by microbial communities, and the primary mediators of methylation determined to date are SRB (Compeau and Bartha, 1985, King et al., 2000), IRB (Fleming et al., 2006), Firmicutes (Gimour et al., 2013), and methanogens (Hamelin et al., 2011, Yu et al., 2012). Thus, the identification and quantification of these microbiota are of significance to this study for their mercury methylation capabilities. *Geobacter* is a

genus of IRB in the class δ -proteobacteria that has demonstrated Hg methylating capabilities (Fleming et al., 2006). *Geobacter* accounted for 22.04% of the δ -proteobacterial abundance at mined sites, and 0.05% at non-mined sites. Results indicate that the abundance of *Geobacter* was significantly higher at mined sites (Kruskal Wallis test, p-value < 0.05). Hg methylation has also been confirmed in a certain member of *Firmicutes*, including certain species of the SRB *Desulfosporosinus* (Gimour et al., 2013). The *Desulfosporosinus* genus accounted for 3.38% of *Firmicute* abundance at mined sites and 0.02% *Firmicute* abundance at non-mined sites. Results demonstrated that *Desulfosporosinus* was significantly higher at mined sites than at non-mined sites (p-value < 0.05). Other known mercury methylating genera identified were *Desulfovibrio*, *Syntrophus*, *Desulfobulbus*, *Desulfitobacterium*, and *Ethanoligenens* and these genera were not present at non-mined sites but were found at mined sites. Overall, it was observed that certain genera of bacteria that contain confirmed mercury methylators were found in significantly higher abundances at mined sites. In conclusion, not only was the sediment microbial community significantly different between mined and non-mined sites, bacteria associated with heavy metal tolerance and bacteria with mercury methylation capabilities were found in higher abundances at mined sites.

Future work

Future work will include identification of *hgcA* and *hgcB* gene homologs among eubacterial, archaeobacterial, and fungal species using bioinformatics analysis (BlastP) and identification of *hgcA* and *hgcB* genes from the genomic DNAs isolated from soil sediments sampled from mined and non-mined sites using PCR. A preliminary analysis of the abundance of *hgcAB*⁺ genera in samples suggests that mined sites have an overall

higher abundance of *hgcAB*⁺ genera, including SRB and IRB. The data shown in Figure 23 supports further investigation into the relationship of *hgcAB*⁺ genera and gold

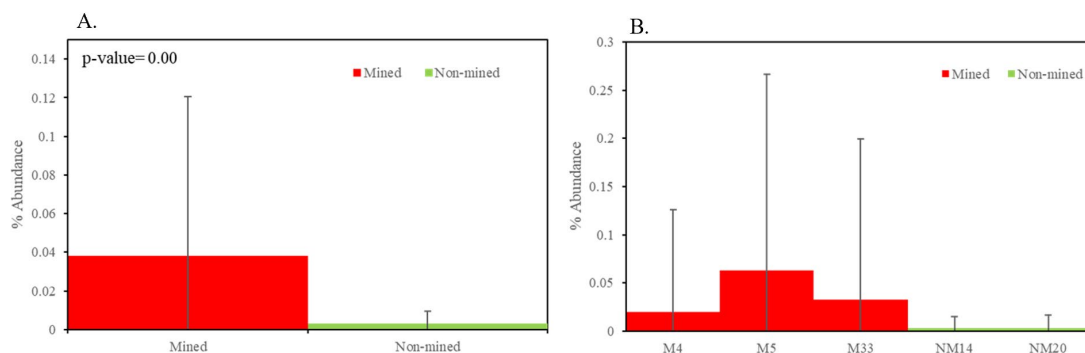


Figure 23. Estimated average (\pm SD) abundance of genera that contain the *hgcAB* gene cluster. Figure 23A. Estimated average abundance of genera for three mined (M) and two non-mined (NM) sites (n=15). Figure 23B. Estimated average abundance of genera for each study sites

mining of the Mazaruni River. In addition to these analyses, analysis of *hgcA* and *hgcB* mRNA expression from bacteria isolated from mined and non-mined sites using RT-PCR and complete microbiome RNA sequencing of bacterial samples obtained from mined and non-mined sites using RNA Seq will be further performed. The cumulative impact of these data will contribute to the development of innovative biomonitoring and bioremediation tools for mercury and its depletion from freshwater ecosystems.

REFERENCES

- Acosta-Martínez, V., Dowd, S., Sun, Y., & Allen, V. (2008). Tag-encoded pyrosequencing analysis of bacterial diversity in a single soil type as affected by management and land use. *Soil Biology and Biochemistry*, 40(11), 2762-2770.
- Albert, J. S., & Reis, R. (Eds.). (2011). *Historical biogeography of Neotropical freshwater fishes*. Univ of California Press, 89-104.
- Allan, J. D., & Castillo, M. M. (2007). Stream ecology: structure and function of running waters. *Springer Science & Business Media*, 388.
- Barakat, M. A. (2011). New trends in removing heavy metals from industrial wastewater. *Arabian journal of chemistry*, 4(4), 361-377.
- Akcil, A., & Koldas, S. (2006). Acid Mine Drainage (AMD): causes, treatment and case studies. *Journal of cleaner production*, 14(12-13), 1139-1145.
- Amoros, C., & Roux, A. L. (1988). Interaction between water bodies within the floodplains of large rivers: function and development of connectivity. *Münstersche Geographische Arbeiten*, 29(1), 125-130.
- Anantharaman, K., Brown, C. T., Hug, L. A., Sharon, I., Castelle, C. J., Probst, A. J., & Brodie, E. L. (2016). Thousands of microbial genomes shed light on interconnected biogeochemical processes in an aquifer system. *Nature communications*, 7, 13219.
- Ayangbenro, A., & Babalola, O. (2017). A new strategy for heavy metal polluted environments: a review of microbial biosorbents. *International journal of environmental research and public health*, 14(1), 94.

- Bae, H. S., Dierberg, F. E., & Ogram, A. (2014). Syntrophs dominate sequences associated with the mercury methylation-related gene *hgcA* in the water conservation areas of the Florida Everglades. *Applied and Environmental Microbiology*, 80(20), 6517-6526.
- Balzino, M., Seccatore, J., Marin, T., De Tomi, G., & Veiga, M. M. (2015). Gold losses and mercury recovery in artisanal gold mining on the Madeira River, Brazil. *Journal of Cleaner Production*, 102, 370-377.
- Barbieri, F. L., & Gardon, J. (2009). Hair mercury levels in Amazonian populations: spatial distribution and trends. *International Journal of Health Geographics*, 8(1), 71.
- Barbieri, F. L., Cournil, A., & Gardon, J. (2009). Mercury exposure in a high fish-eating Bolivian Amazonian population with intense small-scale gold-mining activities. *International Journal of Environmental Health Research*, 19(4), 267-277.
- Barbosa, A. C., De Souza, J., Dorea, J. G., Jardim, W. F., & Fadini, P. S. (2003). Mercury biomagnification in a tropical black water, Rio Negro, Brazil. *Archives of Environmental Contamination and Toxicology*, 45(2), 235-246.
- Barkay, T., & Poulain, A. J. (2007). Mercury (micro) biogeochemistry in polar environments. *FEMS microbiology ecology*, 59(2), 232-241.
- Battarbee, R. W. (1990). The causes of lake acidification, with special reference to the role of acid deposition. *Philosophical Transactions of the Royal Society of London. B, Biological Sciences*, 327(1240), 339-347.

- Battin, T. J. (1998). Dissolved organic matter and its optical properties in a blackwater tributary of the upper Orinoco river, Venezuela. *Organic Geochemistry*, 28(9-10), 561-569.
- Battista, J. R., Earl, A. M., & Park, M. J. (1999). Why is *Deinococcus radiodurans* so resistant to ionizing radiation? *Trends in microbiology*, 7(9), 362-365.
- Berman, M., Chase, T., & Bartha, R. (1990). Carbon flow in mercury biomethylation by *Desulfovibrio desulfuricans*. *Applied and Environmental Microbiology*, 56(1), 298-300.
- Bertoni, C. H., Shaw, R. P., Singh, R., Minamoto, J., Richards, J. M., & Belzile, E. (1991). Geology and gold mineralisation of the Omai property, Guyana. *Brazil gold*, 91, 767-771.
- Beukes, C. W., Palmer, M., Manyaka, P., Chan, W. Y., Avontuur, J. R., van Zyl, E., & Varghese, N. (2017). Genome data provides high support for generic boundaries in *Burkholderia sensu lato*. *Frontiers in microbiology*, 8, 1154.
- Bjørklund, G., Dadar, M., Mutter, J., & Aaseth, J. (2017). The toxicology of mercury: Current research and emerging trends. *Environmental research*, 159, 545-554.
- Börner, F., Gruhne, M., & Schön, J. (1993). Contamination indications derived from electrical properties in the low frequency range 1. *Geophysical Prospecting*, 41(1), 83-98.
- Bradl, H. (Ed.). (2005). *Heavy metals in the environment: origin, interaction and remediation* (Vol. 6). Elsevier.

- Brosse, S., Grenouillet, G., Gevrey, M., Khazraie, K., & Tudesque, L. (2011). Small-scale gold mining erodes fish assemblage structure in small neotropical streams. *Biodiversity and Conservation*, 20(5), 1013-1026.
- Buchanan, S., Anglen, J., & Turyk, M. (2015). Methyl mercury exposure in populations at risk: analysis of NHANES 2011–2012. *Environmental research*, 140, 56-64.
- Budnik, L. T., & Casteleyn, L. (2019). Mercury pollution in modern times and its socio-medical consequences. *Science of The Total Environment*, 654, 720-734.
- Cabral, L., Júnior, G. V. L., de Sousa, S. T. P., Dias, A. C. F., Cadete, L. L., Andreote, F. D., & de Oliveira, V. M. (2016). Anthropogenic impact on mangrove sediments triggers differential responses in the heavy metals and antibiotic resistomes of microbial communities. *Environmental pollution*, 216, 460-469.
- Canterbury, D. C. (2016). Natural resources extraction and politics in Guyana. *The Extractive Industries and Society*, 3(3), 690-702.
- Castro, H. F., Williams, N. H., & Ogram, A. (2000). Phylogeny of sulfate-reducing bacteria. *FEMS Microbiology Ecology*, 31(1), 1-9.
- Chen, Y., Jiang, Y., Huang, H., Mou, L., Ru, J., Zhao, J., & Xiao, S. (2018). Long-term and high-concentration heavy-metal contamination strongly influences the microbiome and functional genes in Yellow River sediments. *Science of the Total Environment*, 637, 1400-1412.
- Christensen, G. A., Wymore, A. M., King, A. J., Podar, M., Hurt, R. A., Santillan, E. U., & Wall, J. D. (2016). Development and validation of broad-range qualitative and clade-specific quantitative molecular probes for assessing mercury methylation in the environment. *Applied and Environmental Microbiology*, 82(19), 6068-6078.

- Chol, K. Y., Satterberg, B., Lyons, D. M., & Elion, E. A. (1994). Ste5 tethers multiple protein kinases in the MAP kinase cascade required for mating in *S. cerevisiae*. *Cell*, 78(3), 499-512.
- Chumchal, M. M., Drenner, R. W., Fry, B., Hambright, K. D., & Newland, L. W. (2008). Habitat-specific differences in mercury concentration in a top predator from a shallow lake. *Transactions of the American Fisheries Society*, 137(1), 195-208.
- Church, C. D., Wilkin, R. T., Alpers, C. N., Rye, R. O., & McCleskey, R. B. (2007). Microbial sulfate reduction and metal attenuation in pH 4 acid mine water. *Geochemical Transactions*, 8(1), 10.
- Clarkson, T. W., & Magos, L. (2006). The toxicology of mercury and its chemical compounds. *Critical reviews in toxicology*, 36(8), 609-662.
- Clifford, M. J. (2011). Pork knocking in the land of many waters: Artisanal and small-scale mining (ASM) in Guyana. *Resources Policy*, 36(4), 354-362.
- Coil, D. A., Neches, R. Y., Lang, J. M., Jospin, G., Brown, W. E., Cavalier, D., & Eisen, J. A. (2019). *Bacterial communities associated with cell phones and shoes* (No. e27514v1). PeerJ Preprints.
- Compeau, G. C., & Bartha, R. (1985). Sulfate-reducing bacteria: principal methylators of mercury in anoxic estuarine sediment. *Applied and Environmental Microbiology*, 50(2), 498-502.
- Cordani, U. G., Teixeira, W., Tassinari, C. C. G., Kawashita, K., & Sato, K. (1988). The growth of the Brazilian Shield. *Episodes*, 11(3), 163-7.

- Date, S. S., Parks, J. M., Rush, K. W., Wall, J. D., Ragsdale, S. W., & Johs, A. (2019). Kinetics of enzymatic mercury methylation at nanomolar concentrations catalyzed by HgcAB. *bioRxiv*, 510180.
- Dedieu, N., Rhone, M., Vigouroux, R., & Céréghino, R. (2015). Assessing the impact of gold mining in headwater streams of Eastern Amazonia using Ephemeroptera assemblages and biological traits. *Ecological Indicators*, *52*, 332-340.
- Depoorter, E., Bull, M. J., Peeters, C., Coenye, T., Vandamme, P., & Mahenthiralingam, E. (2016). *Burkholderia*: an update on taxonomy and biotechnological potential as antibiotic producers. *Applied microbiology and biotechnology*, *100*(12), 5215-5229.
- Demers, J. D., Driscoll, C. T., Fahey, T. J., & Yavitt, J. B. (2007). Mercury cycling in litter and soil in different forest types in the Adirondack region, New York, USA. *Ecological Applications*, *17*(5), 1341-1351.
- Dezécache, C., Faure, E., Gond, V., Salles, J. M., Vieilledent, G., & Hérault, B. (2017). Gold-rush in a forested El Dorado: deforestation leakages and the need for regional cooperation. *Environmental Research Letters*, *12*(3), 034013.
- Dhal, P. K., & Sar, P. (2014). Microbial communities in uranium mine tailings and mine water sediment from Jaduguda U mine, India: a culture independent analysis. *Journal of Environmental Science and Health, Part A*, *49*(6), 694-709.
- Ding, L., Zhao, K., Zhang, L., Liang, P., Wu, S., Wong, M. H., & Tao, H. (2018). Distribution and speciation of mercury affected by humic acid in mariculture sites at the Pearl River estuary. *Environmental pollution*, *240*, 623-629.

- Dittman, J. A., Shanley, J. B., Driscoll, C. T., Aiken, G. R., Chalmers, A. T., Towse, J. E., & Selvendiran, P. (2010). Mercury dynamics in relation to dissolved organic carbon concentration and quality during high flow events in three northeastern US streams. *Water Resources Research*, 46(7).
- Duruibe, J. O., Ogwuegbu, M. O. C., & Ekwurugwu, J. N. (2007). Heavy metal pollution and human biotoxic effects. *International Journal of physical sciences*, 2(5), 112-118.
- Duncan, W. P., & Fernandes, M. N. (2010). Physicochemical characterization of the white, black, and clearwater rivers of the Amazon Basin and its implications on the distribution of freshwater stingrays (Chondrichthyes, Potamotrygonidae). *Pan-American Journal of Aquatic Sciences*, 5(3), 454-464.
- Eagles-Smith, C. A., Silbergeld, E. K., Basu, N., Bustamante, P., Diaz-Barriga, F., Hopkins, W. A., & Nyland, J. F. (2018). Modulators of mercury risk to wildlife and humans in the context of rapid global change. *Ambio*, 47(2), 170-197.
- Ekstrom, E. B., Morel, F. M., & Benoit, J. M. (2003). Mercury methylation independent of the acetyl-coenzyme A pathway in sulfate-reducing bacteria. *Applied and Environmental Microbiology*, 69(9), 5414-5422.
- Esdaile, L. J., & Chalker, J. M. (2018). The Mercury Problem in Artisanal and Small-Scale Gold Mining. *Chemistry—A European Journal*, 24(27), 6905-6916
- Estrada-de los Santos, P., Palmer, M., Chávez-Ramírez, B., Beukes, C., Steenkamp, E., Briscoe, L., & Arrabit, M. (2018). Whole genome analyses suggest that Burkholderia sensu lato contains two additional novel genera (Mycetohabitans

- gen. nov., and *Trinickia* gen. nov.): implications for the evolution of diazotrophy and nodulation in the Burkholderiaceae. *Genes*, 9(8), 389.
- Fieseler, L., Horn, M., Wagner, M., & Hentschel, U. (2004). Discovery of the novel candidate phylum “Poribacteria” in marine sponges. *Applied and Environmental Microbiology*, 70(6), 3724-3732.
- Fergusson, J. E. (1990). *Heavy elements: chemistry, environmental impact and health effects*. Pergamon. 614
- Filippelli, G. M., Morrison, D., & Cicchella, D. (2012). Urban geochemistry and human health. *Elements*, 8(6), 439-444.
- Fleming, E. J., Mack, E. E., Green, P. G., & Nelson, D. C. (2006). Mercury methylation from unexpected sources: molybdate-inhibited freshwater sediments and an iron-reducing bacterium. *Applied and Environmental Microbiology*, 72(1), 457-464.
- Fosmire, G. J. (1990). Zinc toxicity. *The American journal of clinical nutrition*, 51(2), 225-227.
- Fredrickson, J. K., & Gorby, Y. A. (1996). Environmental processes mediated by iron-reducing bacteria. *Current opinion in biotechnology*, 7(3), 287-294.
- Frohne, T., Rinklebe, J., Langer, U., Laing, G. D., Mothes, S., & Wennrich, R. (2012). Biogeochemical factors affecting mercury methylation rate in two contaminated floodplain soils. *Biogeosciences*, 9(1), 493-507.
- García-Sánchez, M., Klouza, M., Holečková, Z., Tlustoš, P., & Száková, J. (2016). Organic and inorganic amendment application on mercury-polluted soils: effects on soil chemical and biochemical properties. *Environmental Science and Pollution Research*, 23(14), 14254-14268.

- Garrity, A. (2006). List of new names and new combinations previously effectively, but not validly, published. *International Journal of Systematic and Evolutionary Microbiology*, 56, 1-6.
- Gilmour, C. C., Podar, M., Bullock, A. L., Graham, A. M., Brown, S. D., Somenahally, A. C., & Elias, D. A. (2013). Mercury methylation by novel microorganisms from new environments. *Environmental science & technology*, 47(20), 11810-11820.
- Grandjean, P., Weihe, P., White, R. F., Debes, F., Araki, S., Yokoyama, K., & Jørgensen, P. J. (1997). Cognitive deficit in 7-year-old children with prenatal exposure to methylmercury. *Neurotoxicology and teratology*, 19(6), 417-428.
- Guallar, E., Sanz-Gallardo, M. I., Veer, P. V. T., Bode, P., Aro, A., Gómez-Aracena, J., & Kok, F. J. (2002). Mercury, fish oils, and the risk of myocardial infarction. *New England Journal of Medicine*, 347(22), 1747-1754.
- Gupta, R. S. (2000). The phylogeny of proteobacteria: relationships to other eubacterial phyla and eukaryotes. *FEMS Microbiology Reviews*, 24(4), 367-402.
- Hall, B. D., Bodaly, R. A., Fudge, R. J. P., Rudd, J. W. M., & Rosenberg, D. M. (1997). Food as the dominant pathway of methylmercury uptake by fish. *Water, Air, and Soil Pollution*, 100(1-2), 13-24.
- Hammond, D. S., Gond, V., De Thoisy, B., Forget, P. M., & DeDijn, B. P. (2007). Causes and consequences of a tropical forest gold rush in the Guiana Shield, South America. *AMBIO: A Journal of the Human Environment*, 36(8), 661-671.
- He, Z. L., Yang, X. E., & Stoffella, P. J. (2005). Trace elements in agroecosystems and impacts on the environment. *Journal of Trace elements in Medicine and Biology*, 19(2-3), 125-140.

- Heulin, T., Barakat, M., Christen, R., Lesourd, M., Sutra, L., De Luca, G., & Achouak, W. (2003). *Ramlibacter tataouinensis* gen. nov., sp. nov., and *Ramlibacter henchirensis* sp. nov., cyst-producing bacteria isolated from sub desert soil in Tunisia. *International journal of systematic and evolutionary microbiology*, 53(2), 589-594.
- Hintelmann, H., Welbourn, P. M., & Evans, R. D. (1995). Binding of methylmercury compounds by humic and fulvic acids. *Water, Air, and Soil Pollution*, 80(1-4), 1031-1034.
- Holum, J. R. (1975). *Elements of general and biological chemistry*. Wiley. 324-469.
- Holt, J. G., Krieg, N. R., Sneath, P. H., Staley, J. T., & Williams, S. T. (1994). *Bergey's manual of determinative bacteriology*. 9th. Baltimore: William & Wilkins.
- Howard, J., Trotz, M. A., Thomas, K., Omisca, E., Chiu, H. T., Halfhide, T., & Stuart, A. L. (2011). Total mercury loadings in sediment from gold mining and conservation areas in Guyana. *Environmental monitoring and assessment*, 179(1-4), 555-573.
- Howard, J. (2010). Mercury in the environment: Field studies from Tampa, Bolivia, and Guyana, 6352.
- Hsu-Kim, H., Kucharzyk, K. H., Zhang, T., & Deshusses, M. A. (2013). Mechanisms regulating mercury bioavailability for methylating microorganisms in the aquatic environment: a critical review. *Environmental science & technology*, 47(6), 2441-2456.
- Hutton, M., & Symon, C. (1986). The quantities of cadmium, lead, mercury and arsenic entering the UK environment from human activities. *Science of the total environment*, 57, 129-150.

- Izagirre, O., Serra, A., Guasch, H., & Elosegi, A. (2009). Effects of sediment deposition on periphytic biomass, photosynthetic activity and algal community structure. *Science of the Total Environment*, 407(21), 5694-5700.
- Jackson, C. R., Millar, J. J., Payne, J. T., & Ochs, C. A. (2014). Free-living and particle-associated bacterioplankton in large rivers of the Mississippi River Basin demonstrate biogeographic patterns. *Applied and Environmental Microbiology*, 80(23), 7186-7195.
- Järup, L. (2003). Hazards of heavy metal contamination. *British medical bulletin*, 68(1), 167-182.
- Kato, S., Sakai, S., Hirai, M., Tasumi, E., Nishizawa, M., Suzuki, K., & Takai, K. (2018). Long-term cultivation and metagenomics reveal ecophysiology of previously uncultivated thermophiles involved in biogeochemical nitrogen cycle. *Microbes and environments*, 17165.
- Kelly, C. A., Rudd, J. W., & Holoka, M. H. (2003). Effect of pH on mercury uptake by an aquatic bacterium: implications for Hg cycling. *Environmental science & technology*, 37(13), 2941-2946.
- Kennish, M. J. (1991). *Ecology of estuaries: anthropogenic effects* (Vol. 1). CRC press.
- Kerin, E. J., Gilmour, C. C., Roden, E., Suzuki, M. T., Coates, J. D., & Mason, R. P. (2006). Mercury methylation by dissimilatory iron-reducing bacteria. *Applied and Environmental Microbiology*, 72(12), 7919-7921.
- Kerrich, R., & Cassidy, K. F. (1994). Temporal relationships of lode gold mineralization to accretion, magmatism, metamorphism and deformation—Archean to present: A review. *Ore Geology Reviews*, 9(4), 263-310.

- Keshri, J., Mankazana, B. B., & Momba, M. N. (2015). Profile of bacterial communities in South African mine-water samples using Illumina next-generation sequencing platform. *Applied microbiology and biotechnology*, *99*(7), 3233-3242.
- Kesse, G. O. (1985). The mineral and rock resources of Ghana. A. Balkema.
- Kim, M. K., & Zoh, K. D. (2012). Fate and transport of mercury in environmental media and human exposure. *Journal of Preventive Medicine and Public Health*, *45*(6), 335.
- King, J. K., Kostka, J. E., Frischer, M. E., & Saunders, F. M. (2000). Sulfate-reducing bacteria methylate mercury at variable rates in pure culture and in marine sediments. *Applied and Environmental Microbiology*, *66*(6), 2430-2437.
- Lacerda, L. D., & Marins, R. V. (1997). Anthropogenic mercury emissions to the atmosphere in Brazil: The impact of gold mining. *Journal of Geochemical Exploration*, *58*(2-3), 223-229. Lacerda, L. D. (1997). Global mercury emissions from gold and silver mining. *Water, Air, and Soil Pollution*, *97*(3-4), 209-221.
- Landrigan, P. J., Schechter, C. B., Lipton, J. M., Fahs, M. C., & Schwartz, J. (2002). Environmental pollutants and disease in American children: estimates of morbidity, mortality, and costs for lead poisoning, asthma, cancer, and developmental disabilities. *Environmental health perspectives*, *110*(7), 721-728.
- Legg, E. D., Ouboter, P. E., & Wright, M. A. P. (2015). Small-scale gold mining related mercury contamination in the Guianas: a review. *World Wildlife Fund: Paramaribo, Suriname*, 61.

- Lenntech Water Treatment and Air Purification (2004). Water Treatment, Published by Lenntech, Rotterdamseweg, Netherlands.
- Lin, H., Hurt Jr, R. A., Johs, A., Parks, J. M., Morrell-Falvey, J. L., Liang, L., & Gu, B. (2014). Unexpected effects of gene deletion on interactions of mercury with the methylation-deficient mutant $\Delta hgcAB$. *Environmental Science & Technology Letters*, 1(5), 271-276
- Järup, L. (2003). Hazards of heavy metal contamination. *British medical bulletin*, 68(1), 167-182.
- Macdonald, K. F. (2016). Impacts of artisanal and large scale gold mining on tropical rivers in West Africa: A case study from the Brong Ahafo Region of Ghana.
- Marszałek, H., & Wąsik, M. (2000). Influence of arsenic-bearing gold deposits on water quality in Złoty Stok mining area (SW Poland). *Environmental Geology*, 39(8), 888-892.
- Marvin-DiPasquale, M. C., & Oremland, R. S. (1998). Bacterial methylmercury degradation in Florida Everglades peat sediment. *Environmental Science & Technology*, 32(17), 2556-2563
- Milési, J. P., Egal, E., Ledru, P., Vernhet, Y., Thiéblemont, D., Cocherie, A., & Lagny, P. H. (1995). Les minéralisations du Nord de la Guyane française dans leur cadre géologique. *Chronique de la recherche minière*, 518, 5-58.
- Mildvan, A. S. (1970). 9 Metals in Enzyme Catalysis. *The enzymes*, 2, 445-536.
- Miller, J. R., Lechler, P. J., & Bridge, G. (2003). Mercury contamination of alluvial sediments within the Essequibo and Mazaruni river basins, Guyana. *Water, Air, and Soil Pollution*, 148(1-4), 139-166.

- Mol, J. H., & Ouboter, P. E. (2004). Downstream effects of erosion from small-scale gold mining on the instream habitat and fish community of a small neotropical rainforest stream. *Conservation Biology*, 18(1), 201-214.
- Morgan, J. N., Berry, M. R., & Graves, R. L. (1997). Effects of commonly used cooking practices on total mercury concentration in fish and their impact on exposure assessments. *Journal of Exposure Analysis and Environmental Epidemiology*, 7(1), 119-133.
- Nagajyoti, P. C., Lee, K. D., & Sreekanth, T. V. M. (2010). Heavy metals, occurrence and toxicity for plants: a review. *Environmental chemistry letters*, 8(3), 199-216.
- Niño-García, J. P., Ruiz-González, C., & del Giorgio, P. A. (2016). Interactions between hydrology and water chemistry shape bacterioplankton biogeography across boreal freshwater networks. *The ISME journal*, 10(7), 1755.
- Nolan K (2003). Copper Toxicity Syndrome, *J. Orthomol. Psychiatry* 12(4): 270 – 282.
- Nriagu, J. O. (1989). A global assessment of natural sources of atmospheric trace metals. *Nature*, 338(6210), 47.
- Nriagu, J., & Becker, C. (2003). Volcanic emissions of mercury to the atmosphere: global and regional inventories. *Science of the Total Environment*, 304(1-3), 3-12.
- Oremland, R. S., Culbertson, C. W., & Winfrey, M. R. (1991). Methylmercury decomposition in sediments and bacterial cultures: involvement of methanogens and sulfate reducers in oxidative demethylation. *Applied and Environmental Microbiology*, 57(1), 130-137.

- Pacyna, E. G., Pacyna, J. M., Steenhuisen, F., & Wilson, S. (2006). Global anthropogenic mercury emission inventory for 2000. *Atmospheric environment*, 40(22), 4048-4063.
- Pais, I., J.B. Jones Jr. The Handbook of Trace Elements, CRC Press, Boca Raton, USA (1997).
- Pak, K. R., & Bartha, R. (1998). Mercury methylation by interspecies hydrogen and acetate transfer between sulfidogens and methanogens. *Applied and Environmental Microbiology*, 64(6), 1987-1990.
- Parkhill, K. L., & Gulliver, J. S. (2002). Effect of inorganic sediment on whole-stream productivity. *Hydrobiologia*, 472(1-3), 5-17.
- Parks, J. M., Johs, A., Podar, M., Bridou, R., Hurt, R. A., Smith, S. D., & Palumbo, A. V. (2013). The genetic basis for bacterial mercury methylation. *Science*, 339(6125), 1332-1335.
- Peppas, A., Komnitsas, K., & Halikia, I. (2000). Use of organic covers for acid mine drainage control. *Minerals Engineering*, 13(5), 563-574.
- Peplow, D. (1999). Environmental impacts of mining in Eastern Washington, center for water and watershed studies fact sheet. *University of Washington*.
- Peplow, D., & Augustine, S. (2014). Neurological abnormalities in a mercury exposed population among indigenous Wayana in Southeast Suriname. *Environmental Science: Processes & Impacts*, 16(10), 2415-2422.
- Pirrone, N., Costa, P., Pacyna, J. M., & Ferrara, R. (2001). Mercury emissions to the atmosphere from natural and anthropogenic sources in the Mediterranean region. *Atmospheric Environment*, 35(17), 2997-3006.

- Pirrone, N., Cinnirella, S., Feng, X., Finkelman, R. B., Friedli, H. R., Leaner, J., & Telmer, K. (2010). Global mercury emissions to the atmosphere from anthropogenic and natural sources. *Atmospheric Chemistry and Physics*, 10(13), 5951-5964.
- Podar, M., Gilmour, C. C., Brandt, C. C., Soren, A., Brown, S. D., Crable, B. R., & Elias, D. A. (2015). Global prevalence and distribution of genes and microorganisms involved in mercury methylation. *Science Advances*, 1(9), e1500675.
- Poulin, J., Gibb, H., Prüss-Üstün, A., & World Health Organization. (2008). Mercury: assessing the environmental burden of disease at national and local levels.
- Pouilly, M., Rejas, D., Pérez, T., Duprey, J. L., Molina, C. I., Hubas, C., & Guimarães, J. R. D. (2013). Trophic structure and mercury biomagnification in tropical fish assemblages, Iténez River, Bolivia. *PloS one*, 8(5), e65054.
- Qiu, G., Feng, X., Li, P., Wang, S., Li, G., Shang, L., & Fu, X. (2008). Methylmercury accumulation in rice (*Oryza sativa* L.) grown at abandoned mercury mines in Guizhou, China. *Journal of agricultural and food chemistry*, 56(7), 2465-2468.
- Rahm, M., Jullian, B., Lauger, A., De Carvalho, R., Vale, L., Totaram, J., & Vieira, R. (2014). Monitoring the impact of gold mining on the forest cover and freshwater in the Guiana Shield. *Reference year*, 60.
- Rakotondrabe, F., Ngoupayou, J. R. N., Mfonka, Z., Rasolomanana, E. H., Abolo, A. J. N., & Ako, A. A. (2018). Water quality assessment in the Bétaré-Oya gold mining area (East-Cameroon): multivariate statistical analysis approach. *Science of the Total Environment*, 610, 831-844

- Ranchou-Peyruse, M., Monperrus, M., Bridou, R., Duran, R., Amouroux, D., Salvado, J. C., & Guyoneaud, R. (2009). Overview of mercury methylation capacities among anaerobic bacteria including representatives of the sulphate-reducers: implications for environmental studies. *Geomicrobiology Journal*, 26(1), 1-8.
- Rastogi, G., Osman, S., Kukkadapu, R., Engelhard, M., Vaishampayan, P. A., Andersen, G. L., & Sani, R. K. (2010). Microbial and mineralogical characterizations of soils collected from the deep biosphere of the former Homestake gold mine, South Dakota. *Microbial ecology*, 60(3), 539-550.
- Ratnaik, R. N. (2003). Acute and chronic arsenic toxicity. *Postgraduate medical journal*, 79(933), 391-396.
- Reddy, Gundlapally S.N. and Pichel, Ferran Garcia. Description of *Patulibacter americanus* sp. nov., isolated from biological soil crusts, emended description of the genus *Patulibacter* Takahashi et al. 2006 and proposal of *Solirubrobacterales* ord. nov. and *Thermoleophilales* ord. nov. *International Journal of Systematic and Evolutionary Microbiology* (2009), 59, 87–94
- Regnell, O., & Watras, C. J. (2018). Microbial Mercury Methylation in Aquatic Environments: A Critical Review of Published Field and Laboratory Studies. *Environmental science & technology*, 53(1), 4-19.
- Rinke, C., Schwientek, P., Sczyrba, A., Ivanova, N. N., Anderson, I. J., Cheng, J. F., & Dodsworth, J. A. (2013). Insights into the phylogeny and coding potential of microbial dark matter. *Nature*, 499(7459), 431.
- Roopnarine, L. (2002). Wounding Guyana: gold mining and environmental degradation. *European Review of Latin American and Caribbean Studies*, (73), 83-91.

- Ruiz-González, C., Niño-García, J. P., Lapierre, J. F., & del Giorgio, P. A. (2015). The quality of organic matter shapes the functional biogeography of bacterioplankton across boreal freshwater ecosystems. *Global ecology and biogeography*, 24(12), 1487-1498.
- Sako, A., Semdé, S., & Wenmenga, U. (2018). Geochemical evaluation of soil, surface water and groundwater around the Tongon gold mining area, northern Cote d'Ivoire, West Africa. *Journal of African Earth Sciences*, 145, 297-316.
- Sandoval, F. (2001). Small-scale mining in Ecuador. *Environment and Society Foundation*, 75.
- Seccatore, J., Veiga, M., Origliasso, C., Marin, T., & De Tomi, G. (2014). An estimation of the artisanal small-scale production of gold in the world. *Science of the Total Environment*, 496, 662-667.
- Sharma, R.K. and Agrawal, M. (2005) Biological Effects of Heavy Metals: An Overview. *Journal of Environmental Biology*, 26, 301-313.
- Smith, S. D., Bridou, R., Johs, A., Parks, J. M., Elias, D. A., Hurt, R. A., & Wall, J. D. (2015). Site-directed mutagenesis of HgcA and HgcB reveals amino acid residues important for mercury methylation. *Applied and Environmental Microbiology*, 81(9), 3205-3217.
- Smith, N. M., Smith, J. M., John, Z. Q., & Teschner, B. A. (2017). Promises and perceptions in the Guianas: The making of an artisanal and small-scale mining reserve. *Resources Policy*, 51, 49-56.

- Spiegel, S. J., Savornin, O., Shoko, D., & Veiga, M. M. (2006). Mercury reduction in Munhena, Mozambique: homemade solutions and the social context for change. *International journal of occupational and environmental health*, 12(3), 215-221.
- Spring, S., Bunk, B., Spröer, C., Schumann, P., Rohde, M., Tindall, B. J., & Klenk, H. P. (2016). Characterization of the first cultured representative of Verrucomicrobia subdivision 5 indicates the proposal of a novel phylum. *The ISME journal*, 10(12), 2801.
- Steckling, N., Tobollik, M., Plass, D., Hornberg, C., Ericson, B., Fuller, R., & Bose-O'Reilly, S. (2017). Global burden of disease of mercury used in artisanal small-scale gold mining. *Annals of global health*, 83(2), 234-247.
- Suárez-Moreno, Z. R., Caballero-Mellado, J., Coutinho, B. G., Mendonça-Previato, L., James, E. K., & Venturi, V. (2012). Common features of environmental and potentially beneficial plant-associated *Burkholderia*. *Microbial Ecology*, 63(2), 249-266.
- Telmer, K. H., & Veiga, M. M. (2009). World emissions of mercury from artisanal and small-scale gold mining. *Mercury fate and transport in the global atmosphere*, 131-172.
- Thomas, C. Y. (2009). Too big to fail: a scoping study of the Small and Medium Scale gold and diamond mining industry in Guyana. *Draft. Georgetown, Guyana*.
- Tchounwou, P. B., Yedjou, C. G., Patlolla, A. K., & Sutton, D. J. (2012). Heavy metal toxicity and the environment. *Molecular, clinical and environmental toxicology*, 133-164.

- Ullrich, S. M., Tanton, T. W., & Abdrashitova, S. A. (2001). Mercury in the aquatic environment: a review of factors affecting methylation. *Critical reviews in environmental science and technology*, 31(3), 241-293.
- UNEP, *UNEP Global Mercury Assessment 2013: Sources, Emissions, Releases and Environmental Transport* (United Nations Environment Programme Chemicals Branch, Geneva, Switzerland, 2013).
- U.S. EPA: 1994, 'Mercury in solid or semisolid waste (manual cold-vapor technique)', Method 7471A. U.S. Environmental Protection Agency, Washington, DC, U.S.A.
- Van der Zaan, B. M., Saia, F. T., Stams, A. J., Plugge, C. M., de Vos, W. M., Smidt, H., Langenhoff, A. A. M., Gerritse, J. (2012). Anaerobic benzene degradation under denitrifying conditions: *Peptococcaceae* as dominant benzene degraders and evidence for a syntrophic process. *Environmental microbiology*, 14(5), 1171-1181.
- Veiga, M. M., Maxson, P. A., & Hylander, L. D. (2006). Origin and consumption of mercury in small-scale gold mining. *Journal of cleaner production*, 14(3-4), 436-447.
- Veiga, M. M., Angeloci, G., Hitch, M., & Velasquez-Lopez, P. C. (2014). Processing centres in artisanal gold mining. *Journal of Cleaner Production*, 64, 535-544.
- Veiga, M. M., Angeloci-Santos, G., & Meech, J. A. (2014). Review of barriers to reduce mercury use in artisanal gold mining. *The Extractive Industries and Society*, 1(2), 351-361.

- Voicu, G., Bardoux, M., & Stevenson, R. (2001). Lithostratigraphy, geochronology and gold metallogeny in the northern Guiana Shield, South America: a review. *Ore Geology Reviews*, 18(3-4), 211-236.
- Ward, J. V. (1989). The four-dimensional nature of lotic ecosystems. *Journal of the North American Benthological Society*, 8(1), 2-8.
- Widdel, F. (1988). Microbiology and ecology of sulfate- and sulfur-reducing bacteria. *Biology of anaerobic microorganisms*, 469-585.
- Yeager, C. M., Dunbar, J., Hesse, C. N., Daligault, H., & Kuske, C. R. (2017). Polysaccharide degradation capability of Actinomycetales soil isolates from a semiarid grassland of the Colorado Plateau. *Applied and Environmental Microbiology*, 83(6), e03020-16.
- Yorifuji, T., Tsuda, T., & Harada, M. (2013). Minamata disease: a challenge for democracy and justice. *Late Lessons from Early Warnings: Science, Precaution, Innovation*. Copenhagen, Denmark: European Environment Agency.
- Yu, R. Q., Reinfelder, J. R., Hines, M. E., & Barkay, T. (2013). Mercury methylation by the methanogen *Methanospirillum hungatei*. *Applied and Environmental Microbiology*, 79(20), 6325-6330.
- Yule, C. M., Boyero, L., & Marchant, R. (2010). Effects of sediment pollution on food webs in a tropical river (Borneo, Indonesia). *Marine and Freshwater Research*, 61(2), 204-213.
- Zhou, J., Riccardi, D., Beste, A., Smith, J. C., & Parks, J. M. (2013). Mercury methylation by HgcA: theory supports carbanion transfer to Hg (II). *Inorganic chemistry*, 53(2), 772-777.

Zwart, G., Crump, B. C., Kamst-van Agterveld, M. P., Hagen, F., & Han, S. K. (2002).

Typical freshwater bacteria: an analysis of available 16S rRNA gene sequences from plankton of lakes and rivers. *Aquatic microbial ecology*, 28(2), 141-155.

APPENDIX A

Collection site, location type (mining or non-mining) and geographic coordinates for all samples (n=81)

Collection site	Location	Geographic coordinates		Collection site	Location	Geographic coordinates		Collection site	Location	Geographic coordinates	
		Latitude	Longitude			Latitude	Longitude			Latitude	Longitude
MAZ-17-04 A	Mining	06.14820°N	060.00514°W	MAZ-17-29 A	Mining	06.20999°N	060.18329°W	MAZ-17-10 A	Non-mining	06.19561°N	060.23248°W
MAZ-17-04 B	Mining	06.14820°N	060.00514°W	MAZ-17-29 B	Mining	06.20999°N	060.18329°W	MAZ-17-10 B	Non-mining	06.19561°N	060.23248°W
MAZ-17-04 C	Mining	06.14820°N	060.00514°W	MAZ-17-29 C	Mining	06.20999°N	060.18329°W	MAZ-17-10 C	Non-mining	06.19561°N	060.23248°W
MAZ-17-05 A	Mining	06.14813°N	060.05128°W	MAZ-17-30 A	Mining	06.20535°N	060.19358°W	MAZ-17-11 A	Non-mining	06.19576°N	060.23230°W
MAZ-17-05 B	Mining	06.14813°N	060.05128°W	MAZ-17-30 B	Mining	06.20535°N	060.19358°W	MAZ-17-11 B	Non-mining	06.19576°N	060.23230°W
MAZ-17-05 C	Mining	06.14813°N	060.05128°W	MAZ-17-30 C	Mining	06.20535°N	060.19358°W	MAZ-17-11 C	Non-mining	06.19576°N	060.23230°W
MAZ-17-07 A	Mining	06.15121°N	060.05845°W	MAZ-17-31 A	Mining	06.10612°N	060.03465°W	MAZ-17-14 A	Non-mining	06.19966°N	060.23640°W
MAZ-17-07 B	Mining	06.15121°N	060.05845°W	MAZ-17-31 B	Mining	06.10612°N	060.03465°W	MAZ-17-14 B	Non-mining	06.19966°N	060.23640°W
MAZ-17-07 C	Mining	06.15121°N	060.05845°W	MAZ-17-31 C	Mining	06.10612°N	060.03465°W	MAZ-17-14 C	Non-mining	06.19966°N	060.23640°W
MAZ-17-08 A	Mining	06.15258°N	060.05802°W	MAZ-17-32 A	Mining	06.11239°N	060.01139°W	MAZ-17-15 A	Non-mining	06.20998°N	060.21540°W
MAZ-17-08 B	Mining	06.15258°N	060.05802°W	MAZ-17-32 B	Mining	06.11239°N	060.01139°W	MAZ-17-15 B	Non-mining	06.20998°N	060.21540°W
MAZ-17-08 C	Mining	06.15258°N	060.05802°W	MAZ-17-32 C	Mining	06.11239°N	060.01139°W	MAZ-17-15 C	Non-mining	06.20998°N	060.21540°W
MAZ-17-23 A	Mining	06.20935°N	060.13413°W	MAZ-17-27 A	Mining	06.21099°N	060.16403°W	MAZ-17-16 A	Non-mining	06.21015°N	060.21569°W
MAZ-17-23 B	Mining	06.20935°N	060.13413°W	MAZ-17-27 B	Mining	06.21099°N	060.16403°W	MAZ-17-16 B	Non-mining	06.21015°N	060.21569°W
MAZ-17-23 C	Mining	06.20935°N	060.13413°W	MAZ-17-27 C	Mining	06.21099°N	060.16403°W	MAZ-17-16 C	Non-mining	06.21015°N	060.21569°W
MAZ-17-24 A	Mining	06.21102°N	060.13611°W	MAZ-17-01 A	Mining	06.21875°N	060.15117°W	MAZ-17-19 A	Non-mining	06.11405°N	060.09004°W
MAZ-17-24 B	Mining	06.21102°N	060.13611°W	MAZ-17-01 B	Mining	06.21875°N	060.15117°W	MAZ-17-19 B	Non-mining	06.11405°N	060.09004°W
MAZ-17-24 C	Mining	06.21102°N	060.13611°W	MAZ-17-01 C	Mining	06.21875°N	060.15117°W	MAZ-17-19 C	Non-mining	06.11405°N	060.09004°W
MAZ-17-25 A	Mining	06.21230°N	060.13836°W	MAZ-17-22 A	Mining	06.20904°N	060.13398°W	MAZ-17-20 A	Non-mining	06.11399°N	060.08991°W
MAZ-17-25 B	Mining	06.21230°N	060.13836°W	MAZ-17-22 B	Mining	06.20904°N	060.13398°W	MAZ-17-20 B	Non-mining	06.11399°N	060.08991°W
MAZ-17-25 C	Mining	06.21230°N	060.13836°W	MAZ-17-22 C	Mining	06.20904°N	060.13398°W	MAZ-17-20 C	Non-mining	06.11399°N	060.08991°W
MAZ-17-26 A	Mining	06.21099°N	060.16451°W	MAZ-17-33 A	Mining	06.11242°N	060.01102°W	MAZ-17-18 A	Non-mining	06.11413°N	060.09022°W
MAZ-17-26 B	Mining	06.21099°N	060.16451°W	MAZ-17-33 B	Mining	06.11242°N	060.01102°W	MAZ-17-18 B	Non-mining	06.11413°N	060.09022°W
MAZ-17-26 C	Mining	06.21099°N	060.16451°W	MAZ-17-33 C	Mining	06.11242°N	060.01102°W	MAZ-17-18 C	Non-mining	06.11413°N	060.09022°W
MAZ-17-28 A	Mining	06.21219°N	060.17082°W	MAZ-17-02 A	Non-mining	06.25096°N	060.14001°W	MAZ-17-21 A	Non-mining	06.11418°N	060.08680°W
MAZ-17-28 B	Mining	06.21219°N	060.17082°W	MAZ-17-02 B	Non-mining	06.25096°N	060.14001°W	MAZ-17-21 B	Non-mining	06.11418°N	060.08680°W
MAZ-17-28 C	Mining	06.21219°N	060.17082°W	MAZ-17-02 C	Non-mining	06.25096°N	060.14001°W	MAZ-17-21 C	Non-mining	06.11418°N	060.08680°W

APPENDIX B

Collection site, location type (mining or non-mining) and geographic coordinates for selected samples (n=15)

Collection site	Location	Geographic coordinates	
		Latitude	Longitude
MAZ-17-04 A	Mining	06.14820°N	060.00514°W
MAZ-17-04 B	Mining	06.14820°N	060.00514°W
MAZ-17-04 C	Mining	06.14820°N	060.00514°W
MAZ-17-05 A	Mining	06.14813°N	060.05128°W
MAZ-17-05 B	Mining	06.14813°N	060.05128°W
MAZ-17-05 C	Mining	06.14813°N	060.05128°W
MAZ-17-33 A	Mining	06.11242°N	060.01102°W
MAZ-17-33 B	Mining	06.11242°N	060.01102°W
MAZ-17-33 C	Mining	06.11242°N	060.01102°W
MAZ-17-14 A	Non-mining	06.19966°N	060.23640°W
MAZ-17-14 B	Non-mining	06.19966°N	060.23640°W
MAZ-17-14 C	Non-mining	06.19966°N	060.23640°W
MAZ-17-20 A	Non-mining	06.11399°N	060.08991°W
MAZ-17-20 B	Non-mining	06.11399°N	060.08991°W
MAZ-17-20 C	Non-mining	06.11399°N	060.08991°W

APPENDIX C

Physical, chemical, and habitat parameters for 17 mined and 10 non-mined sites (n=81)

Classification	Parameters	Mined (M)																Non-mined (NM)										
		2	3	4	5	16	17	18	19	20	21	22	23	24	26	29	32	33	1	7	8	11	12	13	14	15	30	31
	Total Dissolved Solids (mg/L)	2.84	2.8	2.66	2.67	2.81	2.39	2.9	4.17	4	4	3.97	3.05	2.88	4.2	5.83	2.84	2.62	9.57	4.52	4.87	4.7	4.7	4.76	3.07	2.61	3.18	3.09
	Turbidity (NTU)	34.5	27	29.5	32	20.5	40	37	40	31.5	23	20.5	29.5	38.5	35.5	14	20	56.5	11.5	47	39.5	30	40	47	62.5	41.5	111	39.5
	Temperature (°C)	29.6	29.7	33	32.2	29.8	29.5	29	29.3	28	28	27.9	29.6	28.6	28.7	27.6	29.4	28.4	28.3	29.7	27.1	27.8	28.2	27.8	27.4	28.9	27.3	28.1
	Depth (m)	78.1	80.7	71.6	74.1	37.3	78.3	77.3	60.2	92.1	75.6	77.8	68.9	77.3	72.3	78.8	60.2	70.1	28.9	83.5	73.8	79.5	74.1	79.9	79	73	78	66.9
Physical	% Silt	20	40	25	20	30	40	25	10	30	50	30	30	20	20	40	10	40	5	10	50	30	20	20	40	20	10	0
	% Sand	50	50	20	20	40	40	60	40	50	30	10	60	30	30	0	30	20	5	80	20	50	50	60	38	40	20	10
	% Pebble	0	0	20	20	15	10	0	20	0	0	20	0	10	15	0	10	10	0	0	0	0	10	0	0	0	10	5
	% Gravel	20	0	5	10	10	10	0	10	5	0	10	0	10	10	0	30	10	10	0	0	0	0	0	10	0	10	25
	% Cobble	0	0	25	30	0	0	0	10	0	0	10	0	10	10	0	10	0	10	0	0	0	0	0	0	0	15	20
	%Rocks	8	0	0	0	0	0	0	0	0	0	0	0	0	0	10	0	0	50	0	0	0	0	0	0	0	10	20
	Ripples	0	0	0	0	64.5	59.3	98.8	22.9	85.3	21.8	99.8	30.2	98.8	35.4	98.8	12.5	40.6	99.8	94.6	93.6	93.6	0	0	22.9	0	43.7	29.1
	pH	5.81	5.82	5.69	5.59	5.72	5.77	5.9	4.92	4.84	5.05	4.89	5.61	5.64	4.76	6.73	5.88	5.55	6.62	4.7	4.68	4.58	4.64	4.66	5.51	5.43	5.41	5.46
Chemical	Electrical Conductivity (µS/m)	5.66	5.63	5.34	5.35	5.63	5	5.8	8.32	8.01	7.58	7.71	6.02	5.79	8.41	11.64	5.69	5.23	19.23	9.04	9.71	9.42	9.52	9.73	6.14	5.18	6.16	6.17
	Dissolved Oxygen (mg/L)	8.11	7.43	7.2	7.4	7.03	6.65	6.18	6.45	6.45	6.17	6.54	7.83	6.82	6.67	8.89	7.34	8.23	8.95	7.37	8.12	6.7	6.84	6.74	6.76	5.64	6.63	5.57
	% Tress	0	0	5	0	95	90	95	85	80	90	50	85	70	90	90	95	70	85	75	75	90	90	95	75	95	85	96
	% Shrubs	75	90	95	0	5	10	5	10	15	10	30	10	20	10	10	5	20	15	10	20	10	10	5	20	5	10	4
Habitat	% Grass	25	10	0	0	0	0	0	5	5	0	20	5	10	0	0	0	10	0	15	5	0	0	0	5	0	5	0
	% Macrophytes	2	10	5	0	0	0	0	0	0	0	10	0	0	0	0	0	5	0	10	20	0	10	10	5	20	5	10
	% Leaf Litter	0	0	0	0	5	0	10	5	10	10	10	5	10	5	25	10	10	10	0	10	10	5	10	5	10	15	10
	% Woody Debris	0	0	0	0	0	0	5	5	5	10	0	5	10	10	25	0	5	10	0	0	10	5	0	2	10	5	0

APPENDIX D

Physical, chemical, and habitat parameters for three mined and two non-mined sites

(n=15)

Classification	Parameters	Mined			Non-mined	
Sites		4	5	33	14	20
Physical	Total dissolved solids (mg/L)	2.84	2.8	2.62	4.7	2.61
	Turbidity (NTU)	34.5	27	56.5	30	41.5
	Water temperature (°C)	29.6	29.7	28.4	27.8	28.9
	Depth (m)	78.1	80.7	70.1	79.5	73
	%Silt	20	40	40	30	20
	%Sand	50	50	20	50	40
	%Pebbles	0	0	10	0	0
	%Gravel	20	0	10	0	0
	%Cobble	0	0	0	0	0
	%Rocks	8	0	0	0	0
	Ripples	0	0	40.6	93.6	0
Chemical	pH	5.81	5.82	5.55	4.58	5.43
	Electrical conductivity (µS/m)	5.66	5.63	5.23	9.42	5.18
	Dissolved oxygen (mg/L)	8.11	7.43	8.23	6.7	5.64
Habitat	% Trees	0	0	70	90	95
	% Shrubs	75	90	20	10	5
	% Grass	25	10	10	0	0
	% Macrophytes	2	10	5	0	20
	% Leaf litter	0	0	10	10	10
	% Woody debris	0	0	5	10	10

APPENDIX E

Concentrations of Au, As, S, and Hg for 17 mined and 10 non-mined sites (n=81)

Collection site	Location	Au (mg/L)	As (mg/L)	S (mg/kg)	Hg (µg/kg)	Collection site	Location	Au (mg/L)	As (mg/L)	S (mg/kg)	Hg (µg/kg)	Collection site	Location	Au (mg/L)	As (mg/L)	S (mg/kg)	Hg (µg/kg)
MAZ-17-04 A	Mining	< 0.10	< 0.28	4638.26	5.69	MAZ-17-29 A	Mining	< 7.28	< 3.29	1327.47	0.15	MAZ-17-10 A	Non-mining	< 3.51	< 0.33	2098.49	0.03
MAZ-17-04 B	Mining	< 1.15	< 1.30	1952.12	1.72	MAZ-17-29 B	Mining	< 6.24	< 1.77	0.00	0.14	MAZ-17-10 B	Non-mining	< 3.01	< 0.27	1281.56	0.00
MAZ-17-04 C	Mining	< 0.78	< 0.37	1986.08	1.10	MAZ-17-29 C	Mining	< 2.99	< 0.63	1491.13	0.27	MAZ-17-10 C	Non-mining	< 3.13	< 0.31	1236.29	0.00
MAZ-17-05 A	Mining	< 10.39	5.00	0.00	15.66	MAZ-17-30 A	Mining	< 7.29	< 3.77	0.00	1.43	MAZ-17-11 A	Non-mining	< 4.72	< 1.40	5851.94	0.44
MAZ-17-05 B	Mining	< 10.14	4.88	0.00	18.07	MAZ-17-30 B	Mining	< 6.95	< 3.42	1748.19	1.57	MAZ-17-11 B	Non-mining	< 6.61	< 2.10	0.00	3.56
MAZ-17-05 C	Mining	< 10.23	5.26	0.00	13.66	MAZ-17-30 C	Mining	16.50	4.96	476.51	1.97	MAZ-17-11 C	Non-mining	< 5.71	< 1.78	5017.46	4.24
MAZ-17-07 A	Mining	< 3.840	< 1.13	1609.99	4.82	MAZ-17-31 A	Mining	6.93	1.94	2559.19	0.12	MAZ-17-14 A	Non-mining	< 3.605	< 0.64	3257.95	0.11
MAZ-17-07 B	Mining	< 4.55	< 1.53	2888.95	3.01	MAZ-17-31 B	Mining	7.33	1.78	3289.74	0.12	MAZ-17-14 B	Non-mining	< 3.98	< 0.61	2827.46	0.00
MAZ-17-07 C	Mining	< 4.21	< 1.41	2493.17	0.61	MAZ-17-31 C	Mining	6.81	2.07	1931.05	0.24	MAZ-17-14 C	Non-mining	< 4.32	< 0.81	2478.30	0.13
MAZ-17-08 A	Mining	< 1.24	< 0.78	763.19	2.57	MAZ-17-32 A	Mining	13.12	2.53	0.00	0.51	MAZ-17-15 A	Non-mining	< 3.93	< 0.47	1097.27	0.00
MAZ-17-08 B	Mining	< 0.62	< -0.13	3046.18	0.00	MAZ-17-32 B	Mining	9.93	1.97	1649.43	0.47	MAZ-17-15 B	Non-mining	< 4.03	< 0.55	1307.07	0.00
MAZ-17-08 C	Mining	< 0.59	< 0.69	1351.42	0.00	MAZ-17-32 C	Mining	10.75	2.37	0.00	0.48	MAZ-17-15 C	Non-mining	< 3.17	< 0.24	1486.16	0.00
MAZ-17-23 A	Mining	< 5.67	< 0.51	1121.36	0.00	MAZ-17-27 A	Mining	9.49	2.01	1145.21	0.09	MAZ-17-16 A	Non-mining	< 4.04	< 0.38	1387.64	0.00
MAZ-17-23 B	Mining	< 5.85	< 0.87	0.00	0.00	MAZ-17-27 B	Mining	9.97	1.18	0.00	0.14	MAZ-17-16 B	Non-mining	< 3.33	< 0.45	1519.14	0.00
MAZ-17-23 C	Mining	18.49	6.59	0.00	0.00	MAZ-17-27 C	Mining	9.83	1.25	3827.29	0.12	MAZ-17-16 C	Non-mining	< 3.29	< 0.24	1901.28	0.00
MAZ-17-24 A	Mining	< 3.91	< 0.69	2776.69	1.31	MAZ-17-01 A	Mining	18.28	5.72	0.00	2.32	MAZ-17-19 A	Non-mining	< 2.76	< 0.35	1241.08	0.00
MAZ-17-24 B	Mining	< 4.92	< 1.04	0.00	0.32	MAZ-17-01 B	Mining	19.95	6.43	0.00	2.69	MAZ-17-19 B	Non-mining	< 2.77	< 0.17	809.71	0.00
MAZ-17-24 C	Mining	< 5.78	< 1.66	2937.18	0.35	MAZ-17-01 C	Mining	16.86	5.11	0.00	1.41	MAZ-17-19 C	Non-mining	< 2.88	< 0.21	566.21	0.90
MAZ-17-25 A	Mining	< 2.09	< 0.19	1213.22	0.04	MAZ-17-22 A	Mining	11.67	1.844	2281.10	0.15	MAZ-17-20 A	Non-mining	< 2.46	< 0.18	1179.27	0.00
MAZ-17-25 B	Mining	< 2.41	< 0.14	1901.25	0.07	MAZ-17-22 B	Mining	13.53	1.967	0.00	0.13	MAZ-17-20 B	Non-mining	< 2.32	< 0.039	1270.37	0.00
MAZ-17-25 C	Mining	< 4.13	< 0.95	0.00	0.35	MAZ-17-22 C	Mining	10.39	1.053	2637.97	0.10	MAZ-17-20 C	Non-mining	< 2.53	< 0.25	1192.51	0.00
MAZ-17-26 A	Mining	< 3.25	< 0.68	1460.31	0.22	MAZ-17-33 A	Mining	20.26	6.029	327.29	5.98	MAZ-17-18 A	Non-mining	6.21	0.90	0.00	0.06
MAZ-17-26 B	Mining	< 3.05	< 0.20	3335.37	0.24	MAZ-17-33 B	Mining	20.55	6.449	0.00	7.64	MAZ-17-18 B	Non-mining	6.21	0.90	1006.02	0.08
MAZ-17-26 C	Mining	< 1.65	< -0.03	2076.13	0.16	MAZ-17-33 C	Mining	16.29	4.789	0.00	8.00	MAZ-17-18 C	Non-mining	4.96	< 0.50	0.00	0.01
MAZ-17-28 A	Mining	< 3.99	< 1.16	2109.42	0.29	MAZ-17-02 A	Non-mining	< 8.76	7.98	3211.24	5.00	MAZ-17-21 A	Non-mining	5.72	< 0.71	158.30	0.17
MAZ-17-28 B	Mining	< 3.16	< 0.86	2928.99	0.33	MAZ-17-02 B	Non-mining	< 5.23	< 2.38	3872.36	3.83	MAZ-17-21 B	Non-mining	7.82	1.25	1120.33	0.10
MAZ-17-28 C	Mining	< 4.22	< 1.12	1319.21	0.40	MAZ-17-02 C	Non-mining	< 5.91	< 1.83	1801.82	6.81	MAZ-17-21 C	Non-mining	5.75	< 0.75	1403.38	0.09

APPENDIX F

Concentrations of Au, As, S and Hg for three mined and two non-mined sites (n=15)

Collection site	Location	Au (mg/L)	As (mg/L)	S (mg/kg)	Hg (µg/kg)
MAZ-17-04 A	Mining	< 0.10	< 0.28	4638.26	5.69
MAZ-17-04 B	Mining	< 1.15	< 1.30	1952.12	1.72
MAZ-17-04 C	Mining	< 0.78	< 0.37	1986.08	1.10
MAZ-17-05 A	Mining	< 10.39	5.00	0.00	15.66
MAZ-17-05 B	Mining	< 10.14	4.88	0.00	18.07
MAZ-17-05 C	Mining	< 10.23	5.26	0.00	13.66
MAZ-17-33 A	Mining	20.26	6.03	327.29	5.98
MAZ-17-33 B	Mining	20.55	6.45	0.00	7.64
MAZ-17-33 C	Mining	16.29	4.79	0.00	8.00
MAZ-17-14 A	Non-mining	< 3.61	< 0.64	3257.95	0.11
MAZ-17-14 B	Non-mining	< 3.98	< 0.61	2827.46	0.00
MAZ-17-14 C	Non-mining	< 4.32	< 0.81	2478.30	0.13
MAZ-17-20 A	Non-mining	< 2.46	< 0.18	1179.27	0.00
MAZ-17-20 B	Non-mining	< 2.32	< 0.04	1270.37	0.00
MAZ-17-20 C	Non-mining	< 2.53	< 0.25	1192.51	0.00

APPENDIX G

Concentrations of MeHg for three mined and two non-mined sites (n=15)

Collection site	Location	MeHg (ug/kg)
MAZ-17-04 A	Mining	0.26
MAZ-17-04 B	Mining	0.03
MAZ-17-04 C	Mining	0.05
MAZ-17-05 A	Mining	1.46
MAZ-17-05 B	Mining	2.16
MAZ-17-05 C	Mining	1.88
MAZ-17-33 A	Mining	0.41
MAZ-17-33 B	Mining	0.53
MAZ-17-33 C	Mining	0.88
MAZ-17-14 A	Non-mining	0.03
MAZ-17-14 B	Non-mining	0.03
MAZ-17-14 C	Non-mining	0.03
MAZ-17-20 A	Non-mining	0.02
MAZ-17-20 B	Non-mining	0.06
MAZ-17-20 C	Non-mining	0.00

APPENDIX H

Average concentrations of Hg, Au, As, and S across 17 mined and 10 non-mined sites and their p-values (n=81)

	Average (\pm SD)	Average (\pm SD)	
Heavy Metal	Mined	Non-mined	P-value
Hg (μ g/Kg)	2.10 \pm 3.98	0.77 \pm 1.75	0.000
Au (mg/L)	5.23 \pm 7.18	1.22 \pm 2.52	0.009
As (mg/L)	1.5 \pm 2.14	0.37 \pm 1.47	0.001
S (mg/Kg)	1800021.79 \pm 1327273.00	945986.65 \pm 1125478.94	0.004

Average concentrations of Hg, Au, As, and S across three mined and two non-mined sites and their p-values (n=15)

	Average (\pm SD)	Average (\pm SD)	
Heavy Metal	Mined	Non-mined	P-value
Hg (μ g/Kg)	8.61 \pm 5.97	0.04 \pm 0.06	0.001
Au (mg/L)	6.34 \pm 9.59	ND	0.129
As (mg/L)	3.60 \pm 2.75	ND	0.017
S (mg/Kg)	989305.44 \pm 1603408.02	2034310.84 \pm 932398.65	0.072
	Average μ g/Kg (\pm SD)	Average μ g/Kg (\pm SD)	
Organometallic cation	Mined	Non-mined	P-value
MeHg (μ g/Kg)	0.85 \pm 0.80	0.03 \pm 0.03	0.004

APPENDIX I

Average relative abundance (%) of phyla and results of Kruskal Wallis tests for significantly different phyla ($p < 0.05$) between mined and non-mined sites (n=15)

Phylum	Average relative abundance (%)		Kruskal Wallis
	Mined	Non-mined	p-value
Euryarchaeota	0.01	0.00	0.371
Acidobacteria	11.20	8.96	0.556
Actinobacteria	25.78	34.39	0.025
Armatimonadetes	0.20	0.13	0.346
BRC1	0.02	0.00	0.048
Bacteroidetes	2.92	3.74	0.906
Chlamydiae	0.10	0.08	0.289
Chloroflexi	5.12	4.53	0.906
Cloacimonetes	0.01	0.00	0.232
Cyanobacteria	1.07	1.50	0.045
Dadabacteria	0.02	0.00	0.035
Dependentiae	0.17	0.19	0.906
Elusimicrobia	0.21	0.06	0.003
Fibrobacteres	0.03	0.00	0.100
Firestonebacteria	0.00	0.00	0.232
Firmicutes	2.97	4.14	0.239
Fusobacteria	0.01	0.00	0.762
GAL15	0.04	0.03	0.721
Gemmatimonadetes	0.35	0.80	0.637
Latescibacteria	0.02	0.00	0.111
Nitrospinae	0.06	0.01	0.096
Nitrospirae	0.08	0.04	0.195
Patescibacteria	0.36	0.73	0.007
Planctomycetes	0.60	0.96	0.025
Proteobacteria	46.23	34.23	0.001
Rokubacteria	0.08	0.01	0.584
Spirochaetes	0.02	0.00	0.062
Verrucomicrobia	0.37	1.56	0.077
WPS-2	1.78	3.55	0.007
WS4	0.02	0.00	0.128
Bacteria_	0.14	0.37	0.018

APPENDIX J

Average relative abundance (%) of family groups and results of Kruskal Wallis tests for significantly different family groups ($p < 0.05$) between mined and non-mined sites ($n = 15$)

Family	Average relative abundance (%) Kruskal Wallis		
	Mined	Non-mined	p-value
Acetobacteraceae	0.61	0.45	0.409
Azospirillaceae	0.01	0.00	0.340
Inquilinaceae	0.03	0.01	0.724
Caulobacteraceae	1.90	2.08	0.195
Elsteraceae	0.13	0.00	0.001
URHD0088	0.06	0.07	0.636
Elsterales_	1.03	0.79	0.239
Holosporaceae	0.01	0.01	0.848
Micropepsaceae	0.49	0.78	0.025
Paracaeidbacteraceae	0.01	0.05	0.008
Reyranellaceae	0.05	0.05	0.906
Amb-16S-1323	0.03	0.01	0.949
Beijerinckiaceae	3.19	2.08	0.059
Devosiaaceae	0.05	0.02	0.193
Hypohomicrobiaceae	0.53	0.44	0.556
KF-JG30-B3	0.38	0.05	0.005
Methyloligellaceae	0.13	0.12	0.173
Rhizobiaceae	0.12	0.04	0.193
Rhizobiales Incertae Sedis	0.06	0.04	0.768
Rhodomicrobiaceae	0.16	0.37	0.005
Xanthobacteraceae	11.90	9.86	0.637
Rhizobiales_	0.08	0.08	0.556
Magnetospirothaceae	0.32	0.01	0.002
Rhodospirillaceae	0.03	0.02	0.814
Rhodospirillales_	0.01	0.02	0.626
AB1	0.00	0.04	0.001
Mitochondria	0.01	0.02	0.248
Rickettsiaceae	0.00	0.01	0.364
Sphingomonadaceae	1.36	1.39	0.637
Thalassobulales_	0.00	0.00	0.232
Alphaproteobacteria_	0.15	0.16	0.480
Bacteriovoracaceae	0.00	0.01	0.450
Bdellovibrionaceae	0.19	0.27	0.906
DTB120_	0.02	0.00	0.129
Syntrophorhabdaceae	0.04	0.02	0.593
Deltaproteobacteria Incertae Sedis_	0.01	0.00	0.129
Desulfarculaceae	0.02	0.01	0.719
Desulfobulbaceae	0.08	0.00	0.035
Desulfobivibrionaceae	0.13	0.00	0.111
Geobacteraceae	0.94	0.00	0.021
MBNT15_	0.03	0.00	0.017
Archangiaceae	0.36	0.58	0.409
Bifid 19	0.02	0.01	0.385
Haliangiaceae	0.42	0.95	0.005
KD3-10	0.00	0.01	0.894
P30B-42	0.02	0.04	0.195
Phaselocystidaceae	0.02	0.12	0.076
Polyangiaceae	0.43	0.74	0.01
Sandaracinaceae	0.02	0.00	0.006

Family	Average relative abundance (%) Kruskal Wallis		
	Mined	Non-mined	p-value
M1e1-27	0.03	0.05	0.156
Myxococcales_	0.18	0.18	0.723
NB1-j	0.01	0.01	0.619
0319-6G20	0.61	1.84	0.018
Oligoflexaceae	0.06	0.24	0.002
RCP2-54_	0.02	0.02	0.766
SAR324 clade (Marine group B)	0.02	0.00	0.035
uncultured Deltaproteobacterium	0.05	0.01	0.361
Sva0485_	0.05	0.00	0.162
Syntrophaceae	0.08	0.01	0.213
Syntrophobacteraceae	0.09	0.00	0.013
TX1A-33	0.03	0.00	0.017
Beggiatoaceae	0.45	0.00	0.017
A21b	0.16	0.08	0.345
B1-7BS	0.02	0.00	0.307
Burkholderiaceae	13.79	6.06	0.003
Ferrovaceae	0.77	0.00	0.007
Gallionellaceae	0.10	0.00	0.017
Hydrogenophilaceae	0.06	0.01	0.064
Methylophilaceae	0.02	0.00	0.069
Nitrosomonadaceae	0.77	0.15	0.013
Rhodocyclaceae	0.26	0.00	0.013
SC-1-84	0.21	0.02	0.003
Betaproteobacteriales_	0.11	0.01	0.007
Coxiellaceae	0.01	0.03	0.007
Diploricettsiaceae	0.16	0.26	0.077
Enterobacteriaceae	0.00	0.03	0.312
Gammaaproteobacteria Incertae Sedis_	1.38	2.16	0.071
JG36-TzT-191_	0.20	0.46	0.013
Legionellaceae	0.05	0.04	0.513
Methylcocceaceae	0.16	0.00	0.084
Moraxellaceae	0.04	0.03	1.000
Pseudomonadaceae	0.07	0.02	0.361
Solimonadaceae	0.05	0.02	0.155
Steroidobacteraceae	0.20	0.09	0.724
Uncultured Steroidobacter sp	0.01	0.01	0.443
WD260	0.02	0.13	0.001
Rhodanobacteraceae	0.06	0.22	0.003
Xanthomonadaceae	0.00	0.01	0.183
Gammaaproteobacteria_	0.01	0.02	0.187
Proteobacteria_	0.01	0.02	0.187
Methylomirabilaceae	0.02	0.00	0.070
Rokubacteriales_	0.06	0.01	0.456
Spirochaetaceae	0.02	0.00	0.136
Clithoniobacteraceae	0.13	1.41	0.003
Xiphinematobacteraceae	0.01	0.03	0.058
Opitutaceae	0.01	0.01	0.230
Pedosphaeraceae	0.22	0.10	0.126
Uncultured Firmicutes bacterium	0.10	0.34	0.018

VITA

Caroline E. Obkirchner

EDUCATION

Master of Science student in Biology at Sam Houston State University, August 2016 – present. Thesis title: “The effects of gold mining on microbiome composition in a freshwater ecosystem”

Bachelor of Arts (May 2011) in Biology and Music, Cum Laude, at Sam Houston State University, Huntsville, Texas.

EMPLOYMENT

Botany Lab Graduate Teaching Assistant, Department of Biological Sciences, Sam Houston State University, August 2018 – December 2018. Responsibilities include: instructing botany labs and grading.

Genetics Lab Manager, Department of Biological Sciences, Sam Houston State University, August 2017-May 2018. Responsibilities included preparing lab materials (cultures, growth media, plates, etc.) for class and keeping *Drosophila melanogaster* stocks.

Genetics Lab Graduate Teaching Assistant, Department of Biological Sciences, Sam Houston State University, August 2016 – August 2017. Responsibilities include: assisting professors with the preparation and presentation of undergraduate courses, grading, and instructing genetics labs.

Undergraduate Research Assistant, Department of Biological Sciences, Sam Houston State University, May 2016 – August 2016. Responsibilities include: assisting graduate student with preparation of media, taking CFUs and other research lab work.

Private Piano and Voice Teacher, Self Employed, Sam Houston State University, May 2015-August 2015. Responsibilities included lesson planning, teaching student appropriate warm-ups and proper instrumental and voice technique, and increasing student’s repertoire.

Piano Accompanist, Faith Lutheran Church, Huntsville, TX, August 2014-December 2014. Responsibilities included accompanying choir through voice warm ups, learning repertoire and providing accompaniment for choir rehearsals.

PRESENTATIONS AT PROFESSIONAL MEETINGS

Obkirchner, C. E., C. G Montana-Schalk, and M. Choudhary. The effects of gold mining on microbiome composition in a freshwater ecosystem. 2019 Spring Meeting Texas American Society for Microbiology. Oral Presentation.

Obkirchner, C. E., C. G Montana-Schalk, and M. Choudhary. Effects of gold mining activity on freshwater microbiome organization and function. 2017 Fall Meeting Texas American Society for Microbiology. Poster presentation.

Obkirchner, C. E., H. L Johnson, and M. Choudhary. Analysis of Heavy-Metal Related Genes in Bacteria, Texas American Society for Microbiology. 2016 Fall Meeting Texas American Society for Microbiology. Poster presentation.

Obkirchner, C. E., H. L Johnson, and M. Choudhary. A Clean Purple Sweep: Gold Bioremediation Using *Rhodobacter sphaeroides*. Ninth Annual Undergraduate Research Symposium, Sam Houston State University.

RESEARCH EXPERIENCE AND TECHNIQUES

Microbial and Molecular: Skilled in aseptic technique, preparing growth media (solid & liquid), creating bacterial cultures, polymerase chain reaction, gel electrophoresis, DNA extraction and purification.

Analytical: Organic Elemental Analysis (OEA) of soil sediments for Carbon, Hydrogen, Nitrogen & Sulphur, Mercury analysis using Cold Vapor Atomic Absorption Spectroscopy, Gold, Iron, & Arsenic Analysis using Inductively Coupled Plasma Optical Emission Spectroscopy (ICP-OES).

Bioinformatics and Genomics: Familiar with QIIME2, Basic Local Alignment Search Tools including Nucleotide BLAST, Protein BLAST, blastx, tblastn. Codon usage, and promoter analysis

HONORS & ACTIVITIES

- SHSU Music Scholarship recipient 2011-2013
- SHSU Opera Workshop
 - Dido and Aeneas (Soloist)
 - Die Fledermaus (Chorus)
 - Opera Incognito (Chorus)
 - Once Upon and Opera (Soloist)
- 1st Chair All State Soprano 2011